



RESEARCH PAPER

A chalcone derivative, 1m-6, exhibits atheroprotective effects by increasing cholesterol efflux and reducing inflammation-induced endothelial dysfunction

Liv Weichien Chen¹  | Min-Chien Tsai² | Ching-Yuh Chern³ | Tien-Ping Tsao^{1,4} | Feng-Yen Lin^{5,6} | Sy-Jou Chen⁷ | Pi-Fen Tsui⁸ | Yao-Wen Liu¹ | Hsien-Jui Lu³ | Wan-Lin Wu⁹ | Wei-Shiang Lin¹ | Chien-Sung Tsai^{10,11,12} | Chin-Sheng Lin¹ 

¹Division of Cardiology, Department of Medicine, Tri-Service General Hospital, National Defense Medical Center, Taipei, Taiwan

²Department of Physiology and Biophysics, Graduate Institute of Physiology, National Defense Medical Center, Taipei, Taiwan

³Department of Applied Chemistry, National Chiayi University, Chiayi City, Taiwan

⁴Division of Cardiology, Cheng Hsin General Hospital, Taipei, Taiwan

⁵Taipei Heart Research Institute and Department of Internal Medicine, Taipei Medical University, Taipei, Taiwan

⁶Division of Cardiology and Cardiovascular Research Center, Department of Internal Medicine, Taipei Medical University Hospital, Taipei, Taiwan

⁷Department of Emergency Medicine, Tri-Service General Hospital, National Defense Medical Center, Taipei, Taiwan

⁸Graduate Institute of Life Sciences, National Defense Medical Center, Taipei, Taiwan

⁹Department of Molecular Microbiology and Immunology, Keck School of Medicine, University of Southern California, Los Angeles, California, USA

¹⁰Division of Cardiovascular Surgery, Tri-Service General Hospital, National Defense Medical Center, Taipei, Taiwan

¹¹Department and Graduate Institute of Pharmacology, National Defense Medical Center, Taipei, Taiwan

¹²Institute of Pharmacy, I.M. Sechenov First Moscow State Medical University, Moscow, Russia

Correspondence

Chin-Sheng Lin, Division of Cardiology, Tri-Service General Hospital, No. 325, Sec. 2, Cheng-Kung Rd., Neihsu 114, Taipei, Taiwan. Email: littlelincs@gmail.com

Funding information

Taiwan Ministry of Science and Technology, Grant/Award Numbers: MOST 105-2325-B016-001, MOST 106-2314-B-016-038-MY3, MOST 106-2320-B-016-010, MOST 108-3111-Y-016-015; Ministry of National Defense-Medical Affairs Bureau, Grant/Award Numbers: MAB-106-082, MAB-106-102, MAB-109-069; Tri-Service General Hospital, Grant/Award Numbers: TSGH C108-069, TSGH-C107-007-007-S02, TSGH-C108-006-007-007-S02, TSGH-E-109206, TSGH-E-109218

Background and Purpose: Atherosclerosis, resulting from lipid dysregulation and vascular inflammation, causes atherosclerotic cardiovascular disease (ASCVD), which contributes to morbidity and mortality worldwide. Chalcone and its derivatives possess beneficial properties, including anti-inflammatory, antioxidant and antitumour activity with unknown cardioprotective effects. We aimed to develop an effective chalcone derivative with antiatherogenic potential.

Experimental Approach: Human THP-1 cells and HUVECs were used as *in vitro* models. Western blots and real-time PCRs were performed to quantify protein, mRNA and miRNA expressions. The cholesterol efflux capacity was assayed by ³H labelling of cholesterol. LDL receptor knockout (*Ldlr*^{-/-}) mice fed a high-fat diet were used as an *in vivo* atherogenesis model. Haematoxylin and eosin and oil red O staining were used to analyse plaque formation.

Liv Weichien Chen and Min-Chien Tsai contributed equally to this work.

Abbreviations: ABCA1, ATP-binding cassette transporter A1; ABCG1, ATP-binding cassette transporter G1; ApoA1, apolipoprotein A1; ASCVD, atherosclerotic cardiovascular disease; EC, endothelial cell; H&E, haematoxylin and eosin; HUVECs, Human umbilical vein endothelial cells; HFD, high-fat diet; HO-1, haem oxygenase-1; ICAM-1, intercellular adhesion molecule 1; *Ldlr*^{-/-}, LDL receptor knockout; LXRx, liver X receptor- α ; MCP-1, monocyte chemoattractant protein-1; MTT, 3-(4,5-dimethylthiazol-2-yl)-2,5-diphenyltetrazolium bromide; ORO, oil red O; ox-LDL, oxidized LDL; PMA, phorbol 12-myristate 13-acetate; qRT-PCRs, quantitative real-time PCRs; RANTES, regulated on activation, normal T cell expressed and secreted or chemokine (C-C motif) ligand 5; SREBP1, sterol regulatory element-binding protein 1; VCAM-1, vascular cell adhesion molecule 1.

Key Results: Using ATP-binding cassette transporter A1 (ABCA1) expression we identified the chalcone derivative, 1m-6, which enhances ABCA1 expression and promotes cholesterol efflux in THP-1 macrophages. Moreover, 1m-6 stabilizes ABCA1 mRNA and suppresses the expression of potential ABCA1-regulating miRNAs through nuclear factor erythroid 2-related factor 2 (Nrf2)/haem oxygenase-1 (HO-1) signalling. Additionally, 1m-6 significantly inhibits TNF- α -induced expression of adhesion molecules, vascular cell adhesion molecule 1 (VCAM-1) and intercellular adhesion molecule 1 (ICAM-1), plus production of proinflammatory cytokines via inhibition of JAK/STAT3 activation and the modulation of Nrf2/HO-1 signalling in HUVECs. In atherosclerosis-prone mice, 1m-6 significantly reduces lipid accumulation and atherosclerotic plaque formation.

Conclusion and Implications: Our study demonstrates that 1m-6 produces promising atheroprotective effects by enhancing cholesterol efflux and suppressing inflammation-induced endothelial dysfunction, which opens a new avenue for treating ASCVD.

LINKED ARTICLES: This article is part of a themed issue on Risk factors, comorbidities, and comedication in cardioprotection. To view the other articles in this section visit <http://onlinelibrary.wiley.com/doi/10.1111/bph.v177.23/issuetoc>

1 | INTRODUCTION

Atherosclerotic cardiovascular disease (ASCVD) associated with vascular events, such as myocardial infarction, unstable angina, stroke and sudden cardiac death, is the leading cause of mortality and morbidity worldwide (Romaine, Tomaszewski, Condorelli, & Samani, 2015). The critical factors involved in the development of atherosclerosis include lipid dysregulation and endothelial cell (EC) dysfunction. Currently, atherosclerotic cardiovascular disease treatment requires multiple approaches, including antiplatelet agents, β -adrenoceptor antagonists, angiotensin-converting enzyme inhibitors and statins. The development of therapeutic regimens is challenging owing to uncertain atherosclerotic plaque formation mechanisms and the dynamic interactions occurring between plaque and immune cells (Gistera & Hansson, 2017). Accordingly, novel therapeutic strategies should specifically target uncontrolled inflammation and lipid dysregulation in the vessel wall.

Endothelial dysfunction is the initiating event in the progression of atherosclerotic disease (Daiber et al., 2017). Monocytes tightly adhere to endothelial cells, triggering the inflammatory process of atherosclerosis via interactions between integrins and endothelial ligands, such as intercellular adhesion molecule 1 (ICAM-1) and vascular cell adhesion molecule 1 (VCAM-1). In atherosclerosis-prone LDL receptor knockout (*Ldlr*^{-/-}) mice, VCAM-1 depletion significantly reduces the area of early atherosclerotic lesions (Cybulsky et al., 2001). Observational studies of humans have shown that patients with acute coronary syndrome have higher plasma levels of VCAM-1 and ICAM-1 than those without acute coronary syndrome (Macias et al., 2003). Moreover, reverse cholesterol transporters, such as ATP-binding cassette transporter A1

What is already known

- Chalcone derivatives exert anti-inflammatory effects.
- Chalcone derivatives enhance ABCA1 expression in THP-1 macrophages through unclear mechanisms.

What this study adds

- A new chalcone derivative 1m-6 promotes cholesterol efflux, suppressing endothelial dysfunction thus reducing atherosclerosis
- 1m-6 enhances ABCA1 expression and reduces TNF- α -induced adhesion molecules expression in macrophages and HUVECs.

What is the clinical significance

- A novel chalcone derivative with potent atheroprotective effects presents new avenues for treating ASCVD.

(ABCA1) and ATP-binding cassette transporter G1 (ABCG1), export excess cholesterol from peripheral tissues to the liver for subsequent lipid metabolism. Epidemiological studies have identified a negative correlation between cholesterol efflux capacity and cardiovascular events (Khera et al., 2011; Rohatgi et al., 2014). Such evidence points out the critical role of cholesterol efflux and endothelial dysfunction in atherosclerotic cardiovascular disease.

Natural ingredients have been extensively studied for their promising therapeutic effects. Chalcone is a phenolic compound that is present in a wide range of vegetables, fruits, teas and other

plants (Zhuang et al., 2017). Many studies have claimed that chalcones and their derivatives have beneficial pharmaceutical properties, including anti-inflammatory, antioxidant, antiapoptotic and antitumour activity. Chalcone derivatives reduce the LPS-induced inflammatory response in macrophages (Chen et al., 2018). Chalcone derivatives inhibit ischaemia/reperfusion-induced myocardial infarction in rats (Annapurna, Mudagal, Ansari, & Rao, 2012). Additionally, novel synthetic indole-chalcone fibrates exhibit anti-dyslipidaemic effects in hyperlipidaemic rats (Yang et al., 2014). However, the antiatherogenic effects of chalcone derivatives have rarely been mentioned.

We previously demonstrated that a novel chalcone derivative, 1m, up-regulates ABCA1 expression in THP-1 macrophages (Teng et al., 2018). To develop a multifaceted compound for atherosclerotic cardiovascular disease treatment, we identified another novel chalcone derivative, 1m-6, which promotes cholesterol efflux by up-regulating ABCA1 expression in macrophages and attenuates TNF- α -induced endothelial dysfunction. In addition, we evaluated the underlying molecular mechanisms. Undoubtedly, 1m-6 ameliorates atherosclerosis and reduces lipid accumulation in atherosclerosis-prone *Ldlr*^{-/-} mice.

2 | METHODS

2.1 | Chalcone analogue synthesis

Proton (300 MHz) and carbon (75 MHz) NMR spectra were recorded on a Varian Mercury-300 NMR spectrometer (Agilent, Santa Clara, CA, USA). Chemical shifts downfield from tetramethylsilane (TMS), which was used as an internal reference, were reported on the δ scale as parts per million (p.p.m.). Mass spectra were measured using a VG Analytical Model 70–250 s Mass Spectrometer (Varian, Palo Alto, CA, USA). All reagents were used as obtained commercially.

(E)-1-(3,4-dimethoxyphenyl)-3-(4-isopropoxy-3-methoxyphenyl) prop-2-en-1-one (**1m-6**) ¹H-NMR (CDCl₃): δ 7.76 (1H, d, *J* = 15.6 Hz), 7.68 (1H, dd, *J* = 8.7, 1.8 Hz), 7.62 (1H, d, *J* = 1.8 Hz), 7.41 (1H, d, *J* = 15.6 Hz), 7.22 (1H, d, *J* = 8.7 Hz), 6.94 (1H, d, *J* = 8.4 Hz), 6.91 (1H, d, *J* = 8.4 Hz), 4.62 (1H, sept, *J* = 6.0 Hz), 3.97 (6H, s), 3.93 (3H, s), 1.41 (6H, d, *J* = 6.0 Hz); ¹³C-NMR (CDCl₃): δ 188.7, 150.3, 149.8, 149.2, 144.2, 131.6, 128.0, 123.5, 122.8, 122.7, 119.6, 114.6, 111.1, 110.9, 109.9, 71.3, 56.1 (3C), 22.0; EI-MS *m/z* (relative intensity %): 356 (M⁺, 65), 314 (100), 283 (88), 165 (47), 77 (22); HRMS Calcd for C₂₁H₂₄O₅: 356.1624. Found: 356.1627.

2.2 | Reagents and antibodies

Rabbit anti-STAT3 (#8768S, RRID: AB_2722529), rabbit anti-pSTAT3 (#9145S, RRID: AB_2491009), rabbit anti-phospho JAK 2 (pJAK2) primary antibody (#3771, RRID: AB_330403), rabbit anti-JAK2 (#3230, RRID: AB_2128522) and rabbit anti-ICAM-1 primary antibodies (#4915S, RRID: AB_2280018) were obtained from Cell Signaling (Danvers, MA, USA). Rabbit anti-ABCG1 (#NB400-132, RRID: AB_10125717) and rabbit anti-nuclear factor erythroid 2-related

factor 2 (Nrf2 or NRF2) primary antibodies (#NB100-91897, RRID: AB_1217300) were obtained from Novus Biologicals (Littleton, CO, USA). Mouse anti-Histone H1 primary antibody (#05-457, RRID: AB_310843) was obtained from Millipore (Billerica, MA, USA). Mouse anti-ABCA1 (#AB18180, RRID: AB_444302), mouse anti- α -tubulin (#AB7291, RRID: AB_2241126) and rabbit anti-VCAM-1 primary antibodies (#AB134047, RRID: AB_2721053) were obtained from Abcam (Cambridge, UK). Mouse anti-haem oxygenase-1 (HO-1) primary antibody (#sc-136960, RRID: AB_2011613) was obtained from Santa Cruz Biotechnology (Santa Cruz, CA, USA). Mouse anti- β -actin primary antibody (#MA5-15739, RRID: AB_10979409) was obtained from Thermo Scientific (Rockford, IL, USA). Peroxidase-AffiniPure Goat Anti-Mouse IgG (H + L) (#115-035-003, RRID: AB_10015289) and peroxidase-AffiniPure Goat Anti-Rabbit IgG (H + L) secondary antibodies (#111-035-003, RRID: AB_2313567) were obtained from Jackson ImmunoResearch (West Grove, PA, USA). Unless otherwise indicated, other chemicals and reagents were all obtained from Sigma-Aldrich Chemical Company (St. Louis, MO, USA).

2.3 | Cell culture

For human THP-1 macrophage experiments, human THP-1 cells (#60430, RRID: CVCL_0006) were purchased from the Bioresource Collection and Research Centre (Hsinchu, Taiwan) and cultured in RPMI 1640 medium (HyClone, Logan, UT, USA) supplemented with 10% FBS (Gibco, Grand Island, NY, USA), 100 U·ml⁻¹ penicillin (Gibco) and 100 μ g·ml⁻¹ streptomycin (Gibco). At the beginning of the experiments, human THP-1 cells (1 \times 10⁶ cells·ml⁻¹) were differentiated into macrophages by incubation with 100 ng·ml⁻¹ phorbol 12-myristate 13-acetate (PMA) in the culture medium for 3 days. For endothelial cell experiments, human umbilical vein endothelial cells (HUVECs; #2000p-05N, RRID: CVCL_2959) were purchased from Cell Applications (San Diego, CA, USA). The HUVECs were cultured in a mixture of endothelial cell growth medium (Cell Applications, San Diego, CA, USA) and M199 medium (Gibco) supplemented with 20% FBS, 100 U·ml⁻¹ penicillin and 100 μ g·ml⁻¹ streptomycin. Cells at passages 6–7 were used in the experiments.

2.4 | Cell viability assay

The 3-(4,5-dimethylthiazol-2-yl)-2,5-diphenyltetrazolium bromide (MTT) assay was applied to assess cell viability as previously described (Teng et al., 2018). Briefly, THP-1 cells (4 \times 10⁴ cells) were seeded in 96-well plates in the culture medium. The cells were differentiated by treatment with 100 ng·ml⁻¹ PMA for 72 h. After THP-1 cell differentiation, the THP-1-derived macrophages were treated with various concentrations of 1m derivatives (1m-1 to 1m-6) for another 24 h. Subsequently, the cells were washed with culture medium and further incubated with 5 mg·ml⁻¹ MTT at 37°C for 6 h. Then the culture medium was removed and 50- μ l DMSO was added to the wells. Finally, the mitochondrial reduction of MTT, which forms purple formazan dye aggregates, was detected using an ELISA reader (Dynatech Laboratories, West Sussex, UK) at 550-nm absorbance.

2.5 | Western blot assay

The Immuno-related procedures used comply with the recommendations made by the *British Journal of Pharmacology* (Alexander et al., 2018). Enhanced chemiluminescence western blotting was performed as previously described (Chen et al., 2017). THP-1-derived macrophages or HUVECs cultured under the indicated conditions were collected. The collected cells were resuspended in RIPA buffer with protease/phosphatase inhibitors (Roche Diagnostics, Mannheim, Germany). The nucleus lysates were collected using NE-PER™ Nuclear and Cytoplasmic Extraction Reagents (Thermo Scientific; Rockford, IL, USA). The protein concentration was determined using the Bradford assay (Bio-Rad, Hercules CA, USA). Equal amounts of whole-cell extracts were loaded on 10% SDS-PAGE for electrophoresis. Thereafter, proteins were transferred to a nitrocellulose membrane. The membrane was blocked for 1 h with 5% non-fat milk in TBS-T and further incubated with primary antibodies with 2.5% BSA in TBS-T (dilution of 1:5,000 for α -tubulin and β -actin and dilution of 1:1,000 for all others) targeting the indicated proteins overnight at 4°C. Then the membrane was washed three times with TBS-T buffer and incubated for another 1 h with conjugated secondary antibodies at a 1:5,000 dilution in blocking buffer. Finally, after being extensively washed with TBS-T buffer, the membrane was incubated with HRP substrate (Millipore, Billerica, MA, USA) and the signal was acquired by a LAS-4000 Luminescent Image Analyzer (Fujifilm, Tokyo, Japan). The images were analysed using ImageJ software (RRID:SCR_003070, National Institutes of Health, Bethesda, MD, USA). The densitometries of target proteins normalized to internal control were presented.

2.6 | Cholesterol efflux assay

Cells (1×10^6 cells per well) were incubated with $0.5 \mu\text{Ci}\cdot\text{ml}^{-1}$ ^3H -labelled cholesterol (Perkin Elmer) at 37°C for 24 h. After being washed twice with PBS, the cells were treated with 10- μM 1m-6 or 0.05% DMSO for 24 h. Next, the treated cells were incubated for another 2 h in medium containing 2% fatty acid-free BSA (FAFA) and 2- μM acetyl-CoA acetyltransferase inhibitor. Thereafter, 20 $\mu\text{g}\cdot\text{ml}^{-1}$ human apolipoprotein A1 (ApoA1) or BSA was added to the medium and the cells were incubated for another 6 h. Finally, the cells and medium were collected and the radioactivity was measured. The values were expressed as ApoA1 [supernatant-associated ^3H -cholesterol content/total (supernatant-associated + cell-associated) ^3H -cholesterol] – BSA [supernatant-associated ^3H -cholesterol content/total (supernatant-associated + cell-associated) ^3H -cholesterol].

2.7 | Macrophage oil red O staining

Oil red O (ORO; Sigma, St. Louis, MO, USA) staining was applied to measure the lipid accumulation in THP macrophages. THP-1 macrophages were pretreated with 1m-6 or DMSO for 2 h and stimulated with oxidized LDL (ox-LDL) ($50 \mu\text{g}\cdot\text{ml}^{-1}$, Kalen Biomedical, Montgomery Village, MD) for 24 h. The cells were washed with PBS and fixed

with 4% paraformaldehyde, followed by dehydration with 60% isopropanol for 1 min. The lipids were then stained using filtered fresh ORO solution for 15 min at room temperature. Subsequently, haematoxylin was used to counterstain the cell nuclei for 1 min after rinsing with 60% isopropanol. The ORO staining was observed using a light microscope. To quantify the lipid accumulation, the ORO was eluted with 100% isopropanol and measured using a spectrophotometer at 490-nm absorbance.

2.8 | Quantification of mRNA expression

RNA was obtained from cells cultured under the indicated conditions using an RNeasy Mini Kit (#74106, QIAGEN, Hilden, Germany) following the manufacturer's instructions. The concentration and purity of the isolated RNA were evaluated using a Nanodrop spectrophotometer and reverse transcribed to cDNA using an iScript™ cDNA Synthesis Kit (#170-8891, Bio-Rad) following the manufacturer's protocol. Then 5-ng cDNA was amplified in a 20 μl total volume, including KAPA SYBR FAST kit (#kk4609, Kapa Biosystems, Wilmington, MA, USA) components and gene-specific primers, at a final concentration of 100 nM. The cycling program was composed of an initial step to activate the enzyme at 95°C for 3 min, followed by 40 cycles of 95°C for 10 s, 60°C for 20 s and 72°C for 1 s. Finally, after the amplification, the analysis of the melting curve from 65°C to 97°C was performed using a Roche LC480 2X Real-Time PCR system (Roche Diagnostics). Data are presented as the expression of the gene of interest relative to that of an internal control gene (GAPDH) using the comparative CT method. Data are expressed as the relative quantification of target mRNA, which was calculated based on the equation: fold change = $2^{-\Delta(\Delta\text{Ct})}$, where $\Delta\text{Ct} = \text{Ct}_{\text{target gene}} - \text{Ct}_{\text{GAPDH}}$ and $\Delta(\Delta\text{Ct}) = \Delta\text{Ct}_{\text{stimulated}} - \Delta\text{Ct}_{\text{control}}$. The Y axis in figures was labelled as “fold mean of the controls” in all mRNA expression data. The primer sequences are provided in the supporting information (Table S1).

2.9 | Quantification of miRNAs

Cellular miRNAs were obtained from cells cultured in the indicated conditions using a miRNeasy kit (#1038703, Qiagen) following the manufacturer's instructions. A Nanodrop 2000 spectrophotometer (Thermo Scientific) was used to determine the concentration and purity of the isolated RNA. The obtained cDNA was then reverse transcribed from 1 μg of miRNA using a miScript II RT kit with HiFlex Buffer (#218161, Qiagen). Quantitative real-time PCRs (qRT-PCRs) were performed using 20 ng of cDNA mixed with miScript SYBR Green PCR kit components (#218073, Qiagen) and optimized on a Roche LC480 2X (Roche Diagnostics). The cycling program involved initial activation at 95°C for 15 min, followed by 40 cycles of 95°C for 15 s, 55°C for 30 s and 70°C for 30 s. The miRNA expression was analysed by relative quantification with the comparative CT method, normalized to that of RNU6-2 as the universal invariant reference (ΔCt) and compared with that of the vehicle sample ($\Delta\Delta\text{Ct}$). The Y axis in figures was labelled as “fold mean of the controls” in miRNA

expression data. Detailed primer information is provided in the supporting information (Table S2).

2.10 | Enzyme-linked immunosorbent assay (ELISA)

Cytokine concentrations were assayed using DuoSet ELISA kits for the indicated cytokines (R&D Systems; Minneapolis, MN, USA) by following the manufacturer's instructions. Briefly, capture antibodies for the indicated cytokines were coated on a 96-well flat-bottom plate, which was then incubated at room temperature overnight. The coated plate was washed three times with wash buffer. Then the plate was blocked in blocking buffer for 1 h. The standard curve was generated using recombinant proteins diluted twofold in dilution buffer. The collected supernatants were added to each well at the indicated dilutions (5× dilution for IL-6; 10× dilution for IL-8) and incubated for 2 h. After being washed three times, the plate was incubated with detection antibodies for 2 h. Subsequently, the plate was washed, 40×-diluted streptavidin-HRP was added and the plate was incubated for 20 min. Finally, the plate was washed five times, a tetramethylbenzidine substrate solution (Clinical Science Products, Mansfield, MA, USA) was added and the plate was incubated for another 10 min. The reaction was stopped by the addition of a stop solution and the cytokine concentrations were determined at OD450 nm using an ELISA reader (Dynatech Laboratories, West Sussex, UK). Except where stated, all procedures were performed at room temperature.

2.11 | Transient siRNA transfection

To specifically knockdown the expression of the indicated proteins, siHO-1 (#sc-35554) and siCtrl (#sc-37007) were purchased from Santa Cruz Biotechnology and siSTAT3 (#M-003544-02-0005) was purchased from Dharmacon Inc. (Chicago, IL, USA). For THP-macrophage transfection, THP-1 cells were seeded in six-well plates at 80% confluence and differentiated by incubation with 100 ng·ml⁻¹ PMA for 72 h. Dual transfections were performed with 10-nM siHO-1 or siCtrl mixed with Lipofectamine RNAiMAX reagent (Invitrogen, Carlsbad, CA, USA) for 24 h. For HUVEC transfection, the cells were cultured in 35- or 60-mm dishes to 80% confluence. Then the HUVECs were transfected with 10-nM siHO-1, siSTAT3, or siCtrl mixed with Lipofectamine RNAiMAX reagent (Invitrogen) for 24 h. The efficiency of protein knockdown was assessed by western blot.

2.12 | Animals and *in vivo* experiments

All mice used in experiments were bred and maintained in pathogen-free conditions (five mice per cage) under a protocol approved by the Laboratory Animal Center at National Defense Medical Center, Taipei, Taiwan (Approval Number: IACUC-19-012). Animal studies are reported in compliance with the ARRIVE guidelines (Kilkenny, Browne, Cuthill, Emerson, & Altman, 2010) and with the recommendations made by the *British Journal of Pharmacology*. Every effort was

made to minimize animal suffering and the number of animals used. *Ldlr*^{-/-} mice on a C57BL/6J background (RRID: MGI:3772339) were obtained from Professor Shing-Joung Lin's Lab at Taipei Veterans General Hospital in Taiwan. These were selected because deletion of the *Ldlr* gene in mice leads to a remarkable increase in plasma LDL levels and the development of atherosclerotic lesions, which is a widely accepted experimental mouse model to study atherosclerosis (Ishibashi et al., 1993). Mice were housed in a controlled environment at a temperature of 20 ± 2°C, with 50–60% humidity. Mice were exposed to a daily 12-h light–12-h dark cycle with free access to chow diet (13.4% of energy from fat, 60% from carbohydrates, 27.6% from protein, LabDiet 5010, LabDiet, Richmond, IN, USA) and water without restriction. Since gender-dependent responses have been observed in cardiovascular disease models (Patten, 2007), we only included the male mice in our *in vivo* models. Eight-week-old male mice were fed a high-fat diet (HFD) (40% of energy from fat, 43% from carbohydrates, 17% from protein, Product: D02031507, Research Diets, Inc, New Brunswick, NJ, USA) for additional 12 weeks. The mice were randomly grouped into those fed an high-fat diet with DMSO ($n = 6$) and those fed an high-fat diet with 20 mg·kg⁻¹·day⁻¹ 1m-6 ($n = 6$). After 4 weeks of high-fat diet the 12-week-old mice were weighed (27.8 ± 0.6 g) and treated with 1m-6 or DMSO via a subcutaneous ALZET[®] osmotic pump (Alza 10 Co., Palo Alto, CA, USA). Although the study was designed for equal group size of mice from six mated cages, the group sizes become unequal due to unexpected animal deaths during the experiment ($n = 5$ in DMSO group and $n = 6$ in 1m-6 group, respectively). The 20-week-old mice were killed via intraperitoneal (i.p.) injection of a mixture of Zoletil (20 mg·kg⁻¹) and Rompun (5 mg·kg⁻¹), followed by cardiac puncture blood collection (0.8–1 ml per mice). After being perfused with PBS, aortas were collected and fixed in 4% paraformaldehyde for haematoxylin and eosin (H&E), ORO and en face staining.

2.13 | Histological analysis

Collected aortas were fixed in 4% paraformaldehyde for 24 h and then transferred to 30% sucrose PBS buffer for 3 days. Ten-micrometre-thick sections were sliced for further staining. H&E staining (Dako, Glostrup, Denmark) was conducted for morphometric lesion analysis. Furthermore, for neutral lipid detection, 10-µm-thick sections were rinsed with 78% methanol for 1 min and incubated with ORO working solution (Muto Pure Chemicals Co., Ltd. Japan) for 50 min. Next, the sections were rinsed under running tap water for 30 min and mounted on slides. Finally, the slides were examined using a Zeiss LSM780 Laser Scanning Confocal Microscope (Carl Zeiss SAS, Jena, Germany). Unless indicated otherwise, all procedures were performed at room temperature.

2.14 | En face staining of the entire aorta

Aortas were fixed in 4% paraformaldehyde for 2 days before ORO staining (Muto Pure Chemicals). The aortas were excised by cutting through the innominate artery, left common carotid artery and left

subclavian artery, followed by cutting along the inner curvature of the aorta. The flat aortas were fixed on a black plate with pins and imaged within 3 days. Images were captured using an iPhone Xs (Apple Inc., Cupertino, CA, USA).

2.15 | Data and analysis

All experiments were designed to generate groups of equal size, using randomization and blinded analysis. Group sizes in each protocol were determined based on our previous studies, preliminary results and the power analysis (McGrath, Pawson, Sharman, & Alexander, 2015). All the data, including outliers, were included in data analysis and presentation. Data were expressed as the median with individual data. The analysis was interpreted using GraphPad Prism 7 software (RRID: SCR_002798, GraphPad Software Inc., San Diego, CA, USA). Statistical analysis was undertaken only for studies where each group size was at least $n = 5$. The statistical analysis of the two groups was performed using a paired two-tailed Student's *t*-test. The statistical analysis of multiple groups was analysed by one-way ANOVA with Bonferroni's post hoc comparison, which was used only when *F* achieved $P < 0.05$. There was no significant variance in homogeneity. There is only one threshold for statistical significance (<0.05) in all analysis. The declared group size is the number of independent values and the statistical analysis was performed using these independent values. Fold change to control was used in the analysis of gene expressions, including mRNA and miRNA expressions, to avoid the larger variation among different experiments. The mean values of the control group were normalized to 1. The data and statistical analysis comply with the recommendations of the *British Journal of Pharmacology* on experimental design and analysis in pharmacology (Curtis et al., 2018).

2.16 | Nomenclature of targets and ligands

Key protein targets and ligands in this article are hyperlinked to corresponding entries in <http://www.guidetopharmacology.org>, the common portal for data from the IUPHAR/BPS Guide to PHARMACOLOGY (Harding et al., 2018) and are permanently archived in the Concise Guide to PHARMACOLOGY 2019/20 (Alexander et al., 2019).

3 | RESULTS

3.1 | 1m-6 significantly increases cholesterol efflux by increasing ABCA1 expression

We previously revealed that the chalcone derivative, 1m, enhances ABCA1 expression in THP-1 macrophages (Teng et al., 2018). To develop a more potent and multifunctional molecule than 1m, we synthesized six chalcone derivatives: **1m-1** to **1m-6** (Figures S1A and 1a). These aldol intermediates were obtained using a procedure similar to that described previously (Chen et al., 2013). Intramolecular hydrogen bonding, such as that observed in **1m-6**, is known to prevent aldol

reactions. Therefore, 4-isopropoxy-3-methoxybenzaldehyde **C** was used as the starting material for our synthesis. Benzaldehyde **B** was protected with isopropyl bromide and potassium carbonate in dimethylformamide in an approximately 95% yield. The isolated product **B** was then reacted with 1-(3,4-dimethoxyphenyl)ethan-1-one **A** with 5N KOH to produce **1m-6** at an 83% yield (Figure S2). The compound displayed >95% purity based on the $^1\text{H-NMR}$ results (Chen et al., 2013). We further evaluated the biological effects of these new derivatives. We found that 1m-6 was the most potent compound, regulating ABCA1 expression in human THP-1 macrophages (Figure S1). The chemical structure of 1m-6 is shown in Figure 1a. In THP-1 macrophages, after 24 h of treatment with 1m-6, ABCA1 expression significantly increased in a dose-dependent manner; the effect was superior to that of 1m (Figure 1b). Moreover, 1m-6 treatment dose-dependently enhanced ABCA1 mRNA expression (Figure 1c). Western blotting results indicated that treatment with 1m-6 significantly enhanced ABCG1, another vital reverse cholesterol transport, protein expression in THP-1 macrophages (Figure S3). Due to the critical role of ABCA1 and ABCG1 in reverse cholesterol transporter, we further examined the cholesterol efflux capacity of 1m-6-treated THP-1 macrophages. Treatment with 1m-6 significantly increased the cholesterol efflux in THP-1 macrophages (Figure 1d). Moreover, ORO staining was performed to detect macrophage lipid deposition, which revealed that treatment with 1m-6 significantly reduced ox-LDL-induced intracellular lipid accumulation in THP-1 macrophages (Figure 1e). In the MTT assay, there were no apparent cytotoxic effects in THP-1 macrophages treated with 1m-6 at the indicated doses (Figure 1f).

3.2 | 1m-6 enhances ABCA1 expression through the up-regulation of liver X receptor α signalling and down-regulation of the expression of ABCA1-regulating miRNAs

To explore the mechanisms by which 1m-6 affects ABCA1 expression, we examined the effects of 1m-6 on liver X receptor- α (LXR α) signalling. We found that in THP-1 macrophages, 1m-6 significantly up-regulated mRNA expressions of LXR α and ABCA1 after treatment for 6 and 24 h (Figure 2a). We further observed the expression of genes downstream of LXR α signalling and found that in THP-1 macrophages, 1m-6 significantly increased the mRNA expression of ABCG1 and sterol regulatory element-binding protein 1 (SREBP1) and reduced the mRNA expression of monocyte chemoattractant protein-1 (MCP-1). In addition, it regulated, on activation, normal T cell expressed and secreted (RANTES), which are negatively regulated by LXR α (Zelcer & Tontonoz, 2006) (Figure 2a). Additionally, we examined whether 1m-6 participates in the translational modulation of ABCA1. Using actinomycin D to block *de novo* RNA synthesis, we observed that the mRNA of ABCA1 was highly protected from degradation in 1m-6-treated THP-1 macrophages (Figure 2b). Several miRNAs have been shown to be involved in the post-translational regulation of ABCA1 mRNA (Romaine et al., 2015). We found that treatment with 1m-6 significantly reduced expression of miRNAs closely associated with ABCA1

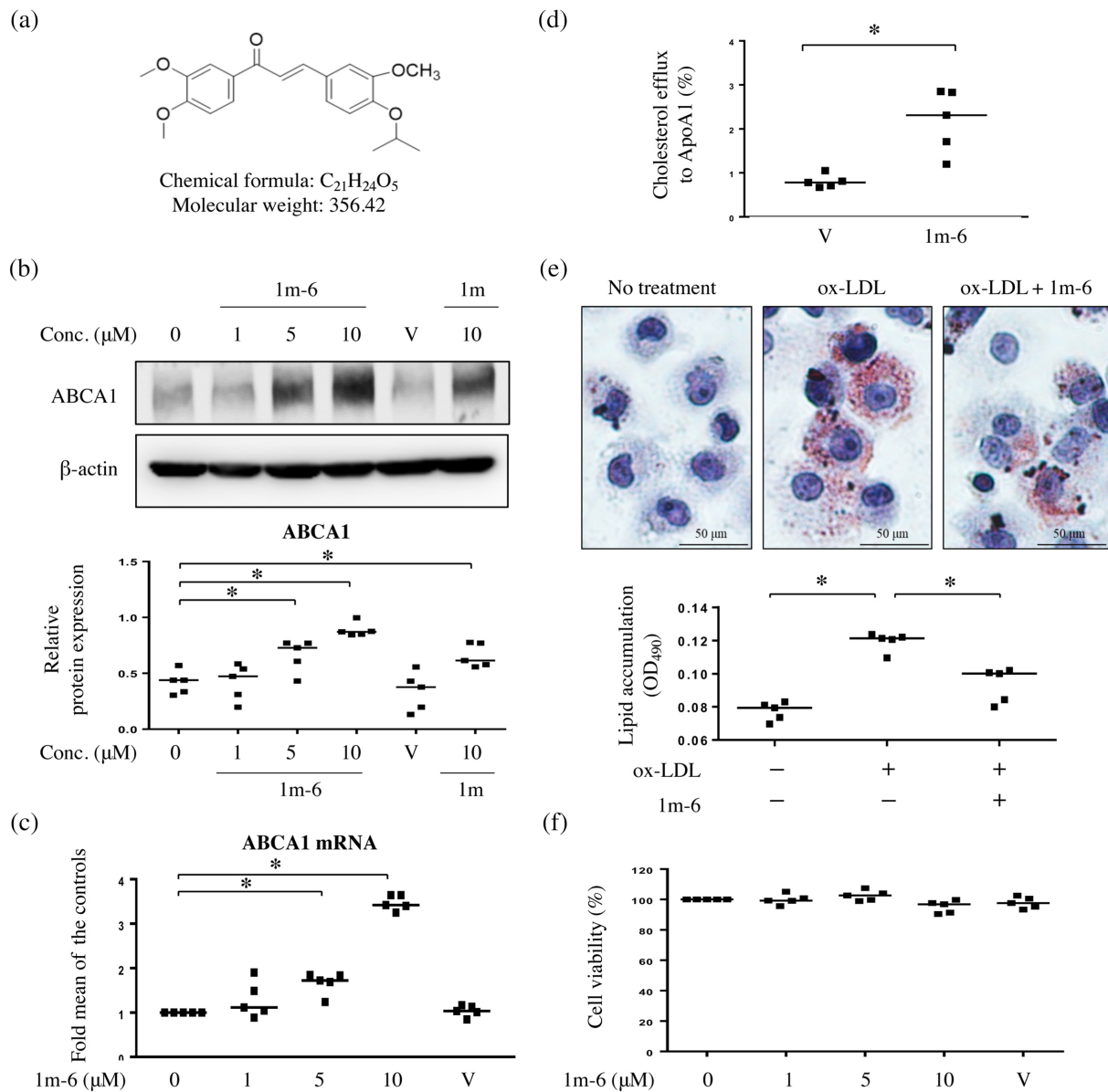


FIGURE 1 A chalcone derivative, 1m-6, significantly increases ATP-binding cassette transporter A1 (ABCA1) expression and promotes cholesterol efflux in THP-1 macrophages. (a) The chemical structure of the chalcone derivative 1m-6. (b) Human THP-1 macrophages were treated with the indicated doses of 1m-6 or 1m for 24 h. Cell lysates were collected and analysed using western blot. Representative data and quantitative results expressed as the median with individual data of five independent experiments are shown. (c) Human THP-1 macrophages were treated with various doses of 1m-6 for 24 h. Cellular RNA was collected for quantitative real-time PCR (qRT-PCR) analysis. Data are shown as the median with individual data of five independent experiments. (d) Total cholesterol efflux was evaluated in THP-1 macrophages treated with 10-μM 1m-6 or DMSO for 24 h after 6 h of incubation with apolipoprotein A1 (ApoA1) or BSA. The results from five independent experiments are presented as the median with individual data. (e) THP-1 macrophages were pretreated with the 1m-6 or DMSO for 2 h and then stimulated with oxidized LDL (ox-LDL) (50 μg·ml⁻¹) for 24 h. Lipids accumulation was determined using oil red O (ORO) staining. The ORO-stained area was observed using light microscopy (400× magnification). Quantitative results were obtained by measuring the eluted ORO using a spectrophotometer. The results from five independent experiments are presented as the median with individual data. (f) Human THP-1 macrophages were treated with various doses of 1m-6 for 24 h and then incubated with 3-(4,5-dimethylthiazol-2-yl)-2,5-diphenyltetrazolium bromide (MTT) for a further 6 h. Cell viability was measured by detecting the absorbance of dissolved MTT crystals using an ELISA reader. The results from five independent experiments are presented as the median with individual data. Conc. indicates concentration. V indicates the vehicle (DMSO) control. Significance is presented as **P* < 0.05 versus the indicated group

regulation, including miR-10b, miR-27a, miR-33, miR-106b, miR-145 and miR-155, though the levels of some ABCA1-regulating miRNAs, such as miR-128, miR-148a, miR-206 and miR-758, were unchanged

or elevated during 1m-6 treatment (Figure 2c). Such evidence partly elucidates that treatment with 1m-6 protected ABCA1 mRNA from degradation. All these results indicate that 1m-6 up-regulates ABCA1

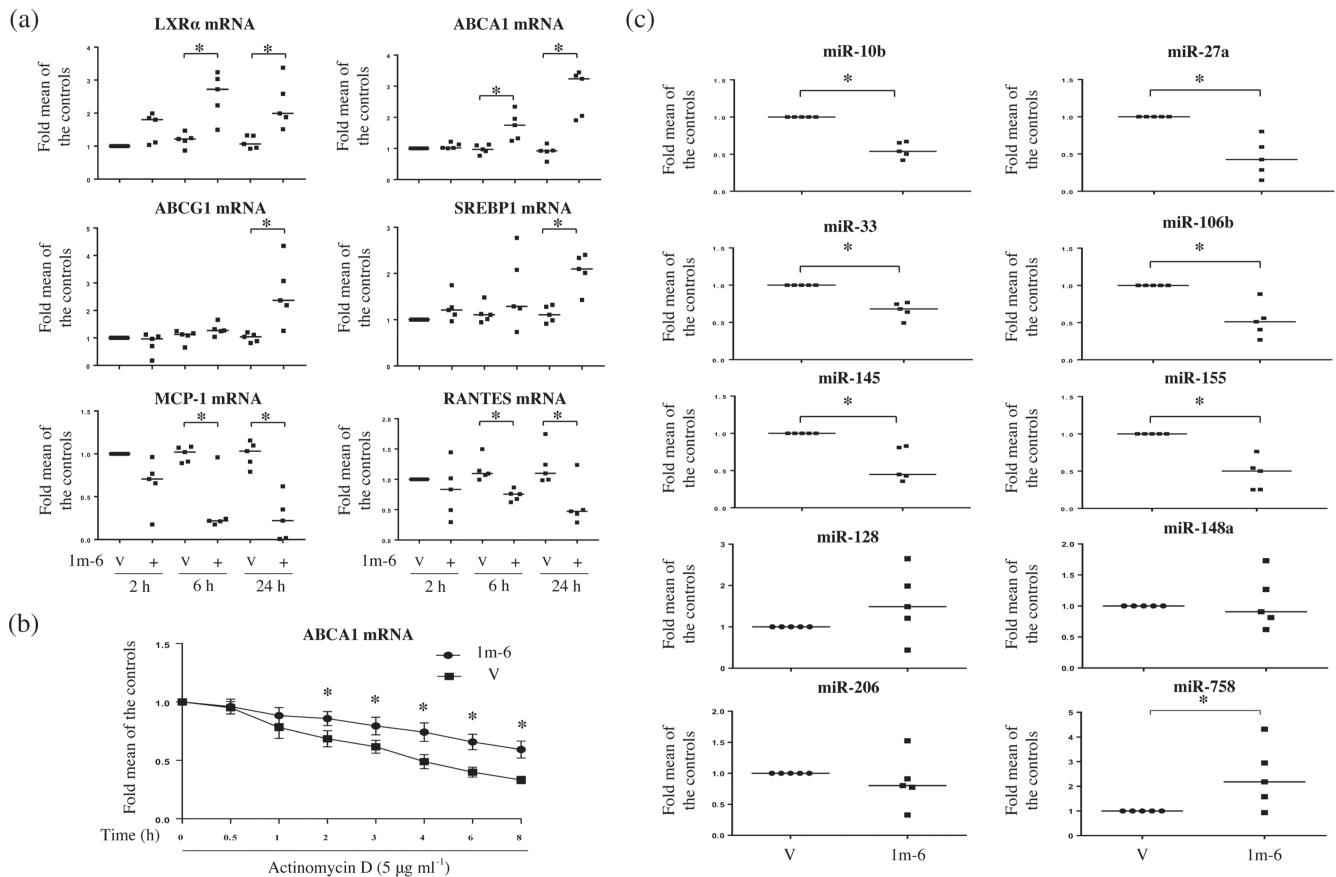


FIGURE 2 1m-6 stabilizes ABCA1 mRNA expression by activating liver X receptor α (LXR α) signalling and reducing the expression of ABCA1-targeting miRNAs in THP-1 macrophages. (a) Human THP-1 macrophages were treated with 10- μM 1m-6 or DMSO for 2, 6, or 24 h. Cellular RNA was collected for qRT-PCR analysis. Data are shown as the median with individual data of five independent experiments. (b) Human THP-1 macrophages were treated with 5 $\mu\text{g}\cdot\text{ml}^{-1}$ actinomycin D and 10- μM 1m-6 or DMSO for the indicated lengths of time. Cellular RNA was collected for qRT-PCR analysis. Data are shown as the mean \pm SEM of six independent experiments. (c) Human THP-1 macrophages were treated with 10- μM 1m-6 or DMSO for 24 h. Cellular miRNA was collected for further qRT-PCR analysis. Data are shown as the median with individual data of five independent experiments. V indicates the vehicle (DMSO) control. Significance is presented as $^*P < 0.05$ versus the indicated group

mRNA expression by activating LXR α signalling and inhibiting miRNA-mediated ABCA1 regulation.

3.3 | 1m-6 promotes ABCA1 expression through Nrf2/HO-1 signalling

It has been reported that chalcone derivatives enhance haem oxygenase-1 (HO-1) expression and anticancer activity in A549 lung cancer cells (Padhye, Ahmad, Oswal, & Sarkar, 2009; Zhao et al., 2017). We found that 1m-6 significantly increased HO-1 expression at both the protein and mRNA levels in THP-1 macrophages (Figure 3a,b). Nrf2 is a key transcription regulator of HO-1 (Itoh et al., 1997; Satoh et al., 2006). We then evaluated the effects of 1m-6 on nuclear Nrf2 expression and found that treatment with 1m-6 significantly enhanced Nrf2 nuclear translocation in THP-1 macrophages (Figure 3c). To evaluate the effects of 1m-6 on the expression of inflammatory cytokines, THP-1 macrophages were treated with 1m-6 before LPS stimulation. We found that LPS enhanced proinflammatory cytokines, including *IL-1 β* , *IL-6* and *TNF- α* ,

mRNA expression. Treatment with 1m-6 further enhanced *IL-1 β* mRNA expression in LPS-induced THP-1 macrophages, while the expressions of *IL-6* and *TNF- α* mRNA exhibited a decreased and no change, respectively (Figure S4). To explore the underlying mechanisms by which HO-1 regulates ABCA1 expression, HO-1 was knocked down in THP-1 macrophages using siRNA treatment. HO-1 silencing significantly reduced the 1m-6-induced HO-1 expression, resulting in inhibition of ABCA1 expression in 1m-6-treated THP-1 macrophages (Figure 3d,e). Moreover, inhibition of HO-1 rescued the 1m-6-induced down-regulation of ABCA1 regulatory miRNAs, including miR-10b, miR-33, miR-106b, miR-145 and miR-155 (Figure 3f). These data highlight that HO-1 plays a pivotal role in the regulation of ABCA1 expression.

3.4 | 1m-6 halts TNF- α -induced endothelial inflammation

TNF- α is known to induce inflammation through the enhanced expression of adhesion molecules and production of proinflammatory

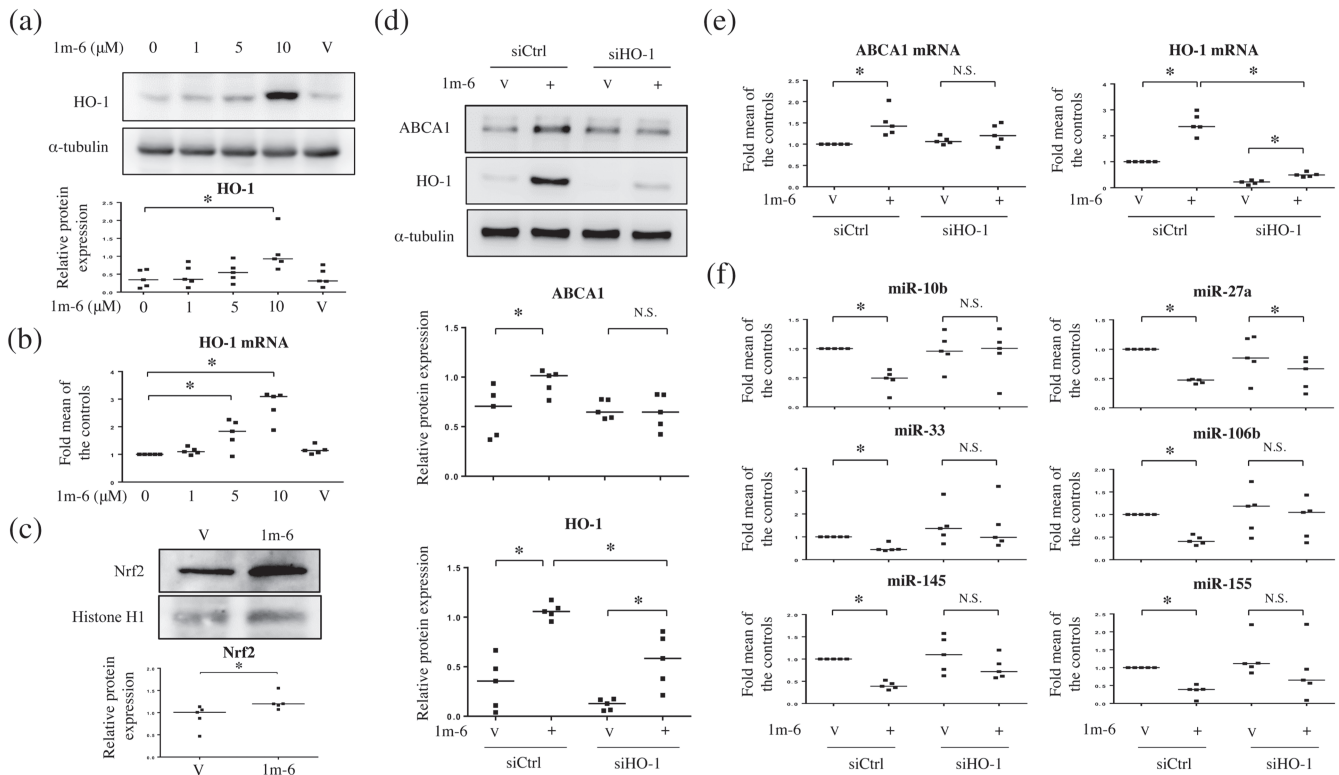


FIGURE 3 1m-6 increases ABCA1 expression through the induction of haem oxygenase-1 (HO-1) expression in THP-1 macrophages. (a and b) Human THP-1 macrophages were treated with the indicated doses of 1m-6 for 24 h. (a) Cell lysates were collected and analysed using western blot. Representative data and quantitative results expressed as the median with individual data of five independent experiments are shown. (b) Cellular mRNA was collected for further qRT-PCR analysis. Data are shown as the median with individual data of five independent experiments. (c) THP-1 macrophages were treated with 1m-6 at the dose of 10 μ M for 24 h. Nuclear lysates were collected and analysed using western blot. Representative data and quantitative results of five independent experiments expressed as the median with individual data are shown. (d–f) THP-1 macrophages were double-transfected with siCtrl or siHO-1 for 24 h. After transfection, the cells were treated with 10- μ M 1m-6 or DMSO for 24 h. (d) Cell lysates were collected and analysed using western blot. Representative data and quantitative results expressed as the median with individual data of five independent experiments are shown. (e) Cellular mRNAs were collected for further qRT-PCR analysis. Data are shown as the median with individual data of five independent experiments. (f) Cellular miRNAs were collected for further qRT-PCR analysis. Data are shown as the median with individual data of five independent experiments. V indicates the vehicle (DMSO) control. Significance is presented as * $P < 0.05$ versus the indicated group. N.S. indicates not significant

cytokines by endothelial cells (Fiedler et al., 2006). In response to TNF- α stimulation, the expression of adhesion molecules, such as VCAM-1 and ICAM-1, was induced in HUVECs (Figure 4a,b). Pre-treatment with 1m-6 significantly suppressed TNF- α -induced expression of VCAM-1 and ICAM-1 at protein and mRNA levels (Figure 4a,b). Additionally, the TNF- α -induced secretion of proinflammatory cytokines, including IL-6 and IL-8 (CXCB8), was inhibited in HUVECs pretreated with 1m-6 (Figure 4c). Furthermore, 1m-6 significantly inhibited TNF- α -induced IL-6 and IL-8 mRNA expression in HUVECs (Figure 4d). These results clearly support the hypothesis that 1m-6 protects against TNF- α -induced endothelial dysfunction.

3.5 | 1m-6 blocks TNF- α -induced ICAM-1 expression through the up-regulation of HO-1 expression

HO-1 exerts anti-inflammatory effects in endothelial cells, such as modulating adhesion molecules and decreasing proinflammatory

cytokine production (Soares et al., 2004). We observed that 1m-6 increases HO-1 expression in THP-1 macrophages (Figure 3), therefore we further examined the effects of 1m-6 on HO-1 expression in HUVECs. Treatment with 1m-6 significantly increased HO-1 protein and mRNA expression in HUVECs (Figure 5a,b). Results demonstrated that treatment with 1m-6 significantly induced nuclear Nrf2 expression in HUVECs (Figure 5c), confirming the effects of 1m-6 on the regulation of Nrf2/HO-1 signalling. To assess the role HO-1 plays in modulating the expression of adhesion molecules, we used siHO-1 to knock down HO-1 expression in 1m-6-treated HUVECs. 1m-6 decreased TNF- α -induced VCAM-1 and ICAM-1 protein expression, and the inhibition of HO-1 neutralized the suppressive effects of 1m-6 on TNF- α -induced ICAM-1, but not VCAM-1, protein expression in HUVECs (Figure 5d). Interestingly, HO-1 silencing did not affect the inhibition of TNF- α -induced ICAM-1 mRNA expression by 1m-6 treatment (Figure 5e). These data suggest that HO-1 plays a role in 1m-6-mediated repression of TNF- α -induced ICAM-1 expression through translational modulation.

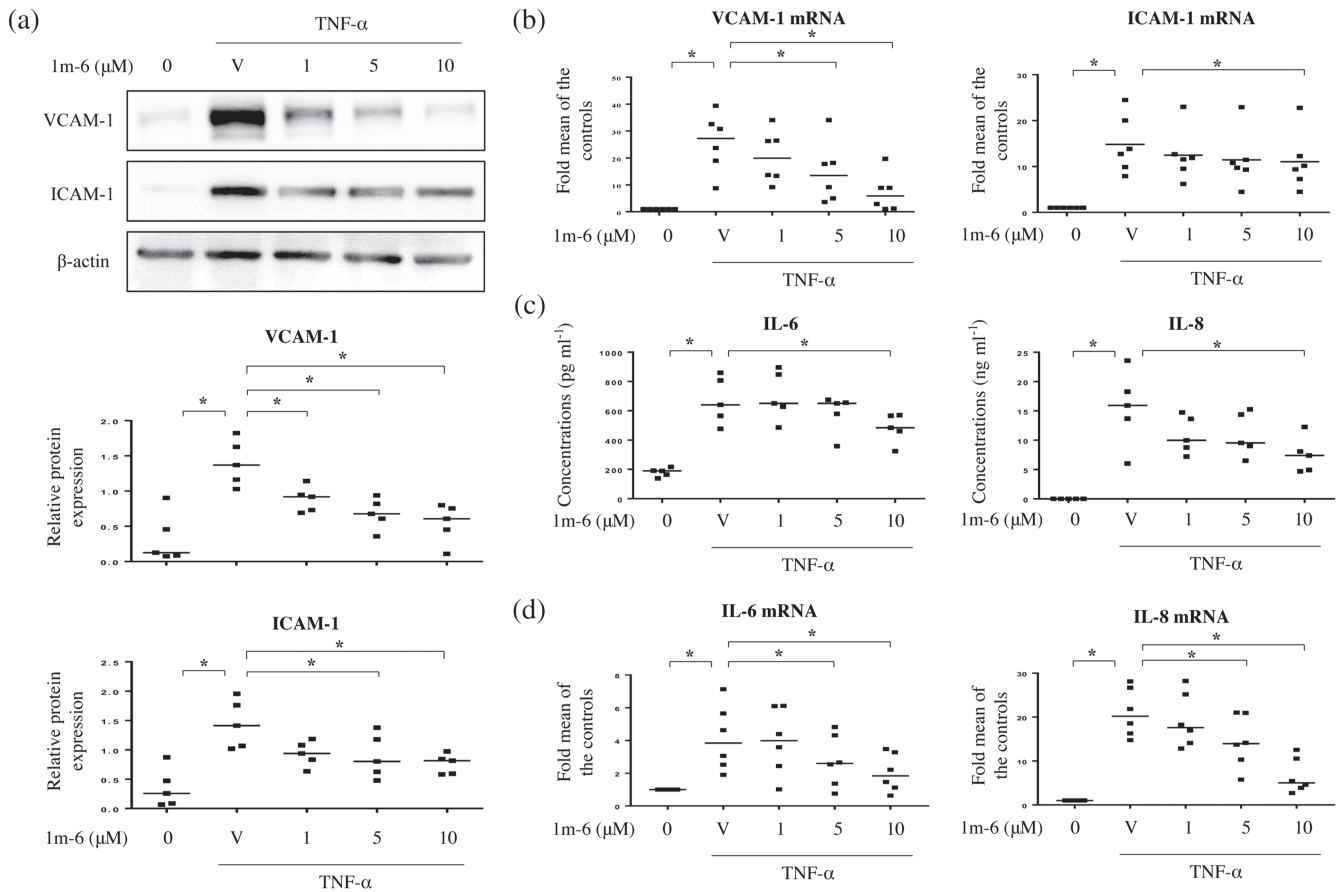


FIGURE 4 1m-6 dose-dependently inhibits the TNF- α -induced production of inflammation mediators in human umbilical vein endothelial cells (HUVECs). HUVECs were pretreated with 1m-6 for 2 h and further stimulated with 10 ng·ml⁻¹ TNF- α for 22 h. (a) Cell lysates were collected and analysed using western blot assay. Representative data and quantitative results expressed as the median with individual data of five independent experiments are shown. (b) Cellular mRNAs were collected for further qRT-PCR analysis. Data are shown as the median with individual data of six independent experiments. (c) Supernatants were collected and analysed using ELISA. Data are shown as the median with individual data of five independent experiments. (d) Cellular mRNAs were collected for qRT-PCR analysis. Data are shown as the median with individual data of six independent experiments. V indicates the vehicle (DMSO) control. Significance is presented as * P < 0.05 versus the indicated group

3.6 | 1m-6 suppresses TNF- α -induced VCAM-1 expression via inhibition of JAK/STAT3 signalling

To explore the regulation of VCAM-1 expression in 1m-6-treated HUVECs, we analysed the effects of 1m-6 treatment on TNF- α -activated NF- κ B signalling. We found that 1m-6 treatment did not affect NF- κ B signalling activation in TNF- α -activated HUVECs (Figure S5). Previous studies have shown that STAT3 signalling is involved in the modulation of TNF- α -induced adhesion molecule expression (Lee et al., 2012). Treatment with TNF- α activated STAT3 at the time points of 2 and 4 h, whereas treatment with 1m-6 significantly decreased STAT3 activation (Figure 6a). We further found that pretreatment with 1m-6 dose-dependently inhibited TNF- α -induced STAT3 phosphorylation in HUVECs (Figure 6b). Previous studies suggested that TNF- α activates the JAK pathway, leading to persistent phosphorylation of STAT3 in HUVECs (Kandhaya-Pillai et al., 2017). To evaluate the regulatory mechanism of 1m-6 on STAT3 phosphorylation, we investigated the activities of JAK2 and found

that treatment with 1m-6 significantly reduced TNF- α -enhanced JAK2 phosphorylation (Figure 6c). Such results clearly elucidate the effects of 1m-6 on the JAK/STAT3 signalling pathway. Moreover, the inhibition of STAT3 by siRNA significantly suppressed TNF- α -induced VCAM-1 expression at protein and RNA levels (Figure 6d,e). These results suggest that 1m-6 inhibits TNF- α -induced VCAM-1 expression through JAK/STAT3 signalling.

3.7 | Treatment with 1m-6 ameliorates arterial plaque formation and lipid accumulation in atherosclerosis-prone mice

Ldlr^{-/-} mice, which are prone to developing atherosclerosis, were fed a high-fat diet and treated with 1m-6 or vehicle via subcutaneous mini-pump. Light microscopy analysis showed that, compared to DMSO treatment, 1m-6 treatment reduced plaque formation in the aortic arch (Figure 7a). Moreover, en face ORO staining of the whole aorta showed significantly decreased lipid content in the 1m-6-treated

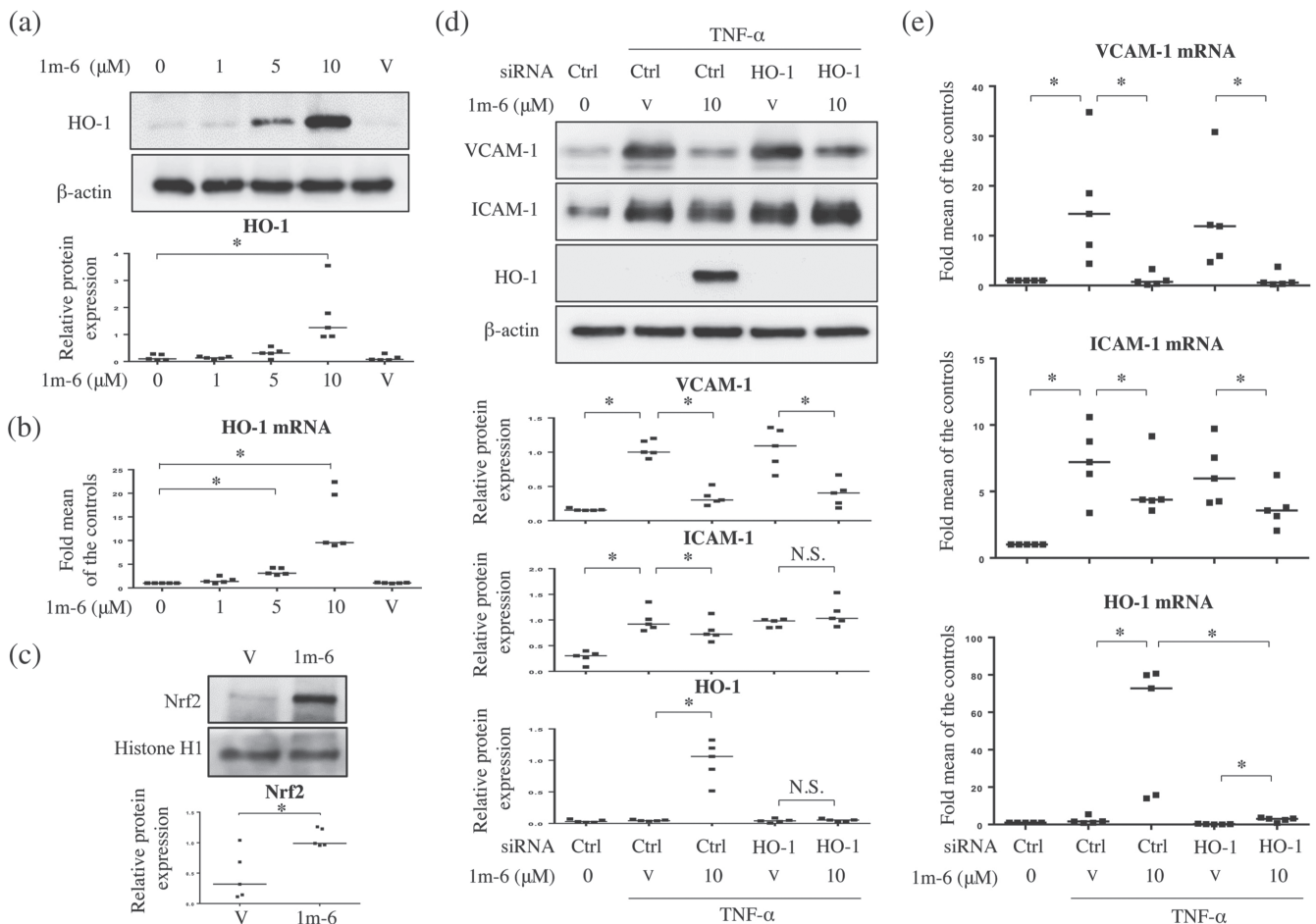


FIGURE 5 1m-6 blocks TNF- α -induced intercellular adhesion molecule 1 (ICAM-1) expression by inducing HO-1 expression in human umbilical vein endothelial cells (HUVECs). (a and b) HUVECs were treated with various doses of 1m-6 for 24 h. (a) Cell lysates were collected and analysed using western blot. Representative data and quantitative results expressed as the median with individual data of five independent experiments are shown. (b) Supernatants were collected and analysed using ELISAs. Data are shown as the median with individual data of five independent experiments. (c) HUVECs were treated with 10- μ M 1m-6 for 24 h. Nuclear lysates were collected and analysed using western blot. Representative data and quantitative results of five independent experiments expressed as the median with individual data are shown. (d and e) HUVECs were transiently transfected with siCtrl or siHO-1 for 24 h. After transfection, the cells were treated with 10- μ M 1m-6 or DMSO for 2 h and further stimulated with 10 ng·ml⁻¹ TNF- α for 22 h. (d) Cell lysates were collected and analysed using western blot. Representative data and quantitative results expressed as the median with individual data of five independent experiments are shown. (e) Cellular mRNA was collected for further qRT-PCR analysis. Data are shown as the median with individual data of five independent experiments. V indicates the vehicle (DMSO) control. Significance is presented as * $P < 0.05$ versus the indicated group. N.S. indicates non-significant

group (Figure 7b). The morphological pictures of the brachiocephalic artery from 1m-6- and DMSO-treated mice are shown in Figure 7c. Lipid deposition in the brachiocephalic artery was examined by ORO staining (Figure 7d). Compared to the DMSO-treated group, the 1m-6-treated groups showed significantly reduced plaque formation and lipid accumulation in the brachiocephalic artery (Figure 7c,d). These data suggest that 1m-6 has therapeutic potential in atherosclerosis-prone mice.

4 | DISCUSSION AND CONCLUSIONS

In the current study, we demonstrate that a novel synthetic chalcone derivative, 1m-6, facilitates cholesterol efflux by up-regulating ABCA1 expression through the activation of LXR α -ABCA1 and Nrf2/HO-1

signalling to suppress the miRNA-mediated regulation of ABCA1 expression in THP-1 macrophages. Additionally, 1m-6 rescues inflammation-mediated endothelial dysfunction by modulating Nrf2/HO-1 and JAK/STAT3 signalling in TNF- α -activated HUVECs. Promisingly, 1m-6 attenuates atherosclerotic plaque and lipid accumulation in the arteries of atherosclerosis-prone mice (Figure 8).

ABCA1 plays a vital role in the efflux of cholesterol from cells to ApoA1 (Phillips, 2014). Both transcriptional and post-translational regulation play a crucial role in the control of its expression (Canfran-Duque, Ramirez, Goedeke, Lin, & Fernandez-Hernando, 2014). LXR α signalling induces the expression of many genes involved in cholesterol transport, including ABCA1 and ABCG1. In the current study, 1m-6 treatment was found to highly up-regulate LXR α , ABCA1 and ABCG1 gene expression. In addition, 1m-6 increased the

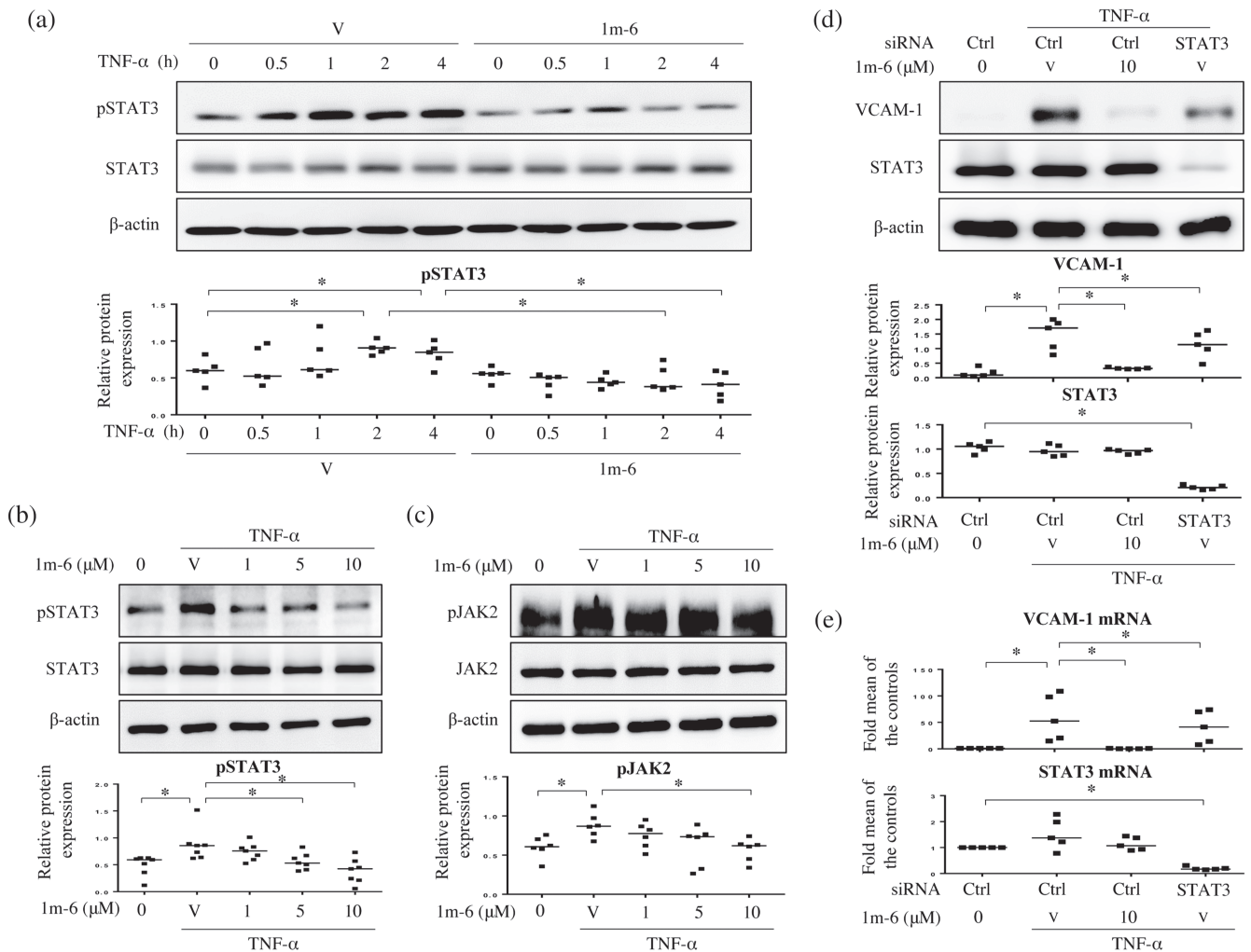


FIGURE 6 1m-6 suppresses TNF- α -induced vascular cell adhesion molecule 1 (VCAM-1) expression through the inhibition of STAT3 signalling. (a) Human umbilical vein endothelial cells (HUVECs) were pretreated with 10- μ M 1m-6 or DMSO for 2 h and further stimulated with 10 ng ml⁻¹ TNF- α for the indicated time points. Cell lysates were collected and analysed using western blot. Representative data and quantitative results expressed as the median with individual data of five independent experiments are shown. (b) HUVECs were pretreated with various doses of 1m-6 or DMSO for 2 h and further stimulated with 10 ng ml⁻¹ TNF- α for 2 h. Cell lysates were collected and analysed using western blot. Representative data and quantitative results expressed as the median with individual data of seven independent experiments are shown. (c) HUVECs were pretreated with various doses of 1m-6 or DMSO for 2 h and then stimulated with 10 ng ml⁻¹ of TNF- α for 30 min. Cell lysates were collected and analysed using western blot. Representative data and quantitative results of six independent experiments expressed as the median with individual data are shown. (d and e) HUVECs were transiently transfected with siCtrl or siSTAT3 for 24 h. After transfection, the cells were pretreated with 10- μ M 1m-6 or DMSO for 2 h and further stimulated with 10 ng ml⁻¹ TNF- α for 22 h. (d) Cell lysates were collected and analysed using western blot. Representative data and quantitative results expressed as the median with individual data of five independent experiments are shown. (e) Cellular mRNAs were collected for further qRT-PCR analysis. Data are shown as the median with individual data of five independent experiments. V indicates the vehicle (DMSO) control. Significance is presented as * $P < 0.05$ versus the indicated group

expression of the *SREBP1* gene, which contains the LXR α response elements in its promoter (Ma et al., 2008). Moreover, anti-inflammatory LXR signalling has been shown to suppress the expression of proinflammatory genes, including *MCP-1* and *RANTES* (Bensinger & Tontonoz, 2008). The anti-inflammatory properties of 1m-6 were shown by its negative regulation of *MCP-1* and *RANTES* in THP-1 macrophages. These results indicate that 1m-6 positively regulates LXR α signalling to enhance *ABCA1* transcription and protect against atherosclerosis.

Regarding the post-translational regulation, there is a long 3'-UTR in *ABCA1* with many miRNA binding sites (Ramirez

et al., 2011). Previous studies have shown that several miRNAs, including miR-33, miR-27a, miR-10b, miR-145 and miR-155, are involved in the post-translational regulation of *ABCA1* biosynthesis (Canfran-Duque, Lin, Goedeke, Suarez, & Fernandez-Hernando, 2016; Kang et al., 2013; Price et al., 2019). Therapeutic interventions promoting *ABCA1*-dependent cholesterol efflux have been shown to halt atherosclerosis by reducing the expression of miRNAs, mainly miR-33, followed by miR-19b and miR-122 (Baselga-Escudero et al., 2014; Lv et al., 2015). These compounds, including diosgenin, enhance *ABCA1* expression through the suppression of one or two miRNAs. Our study clearly demonstrates that 1m-6

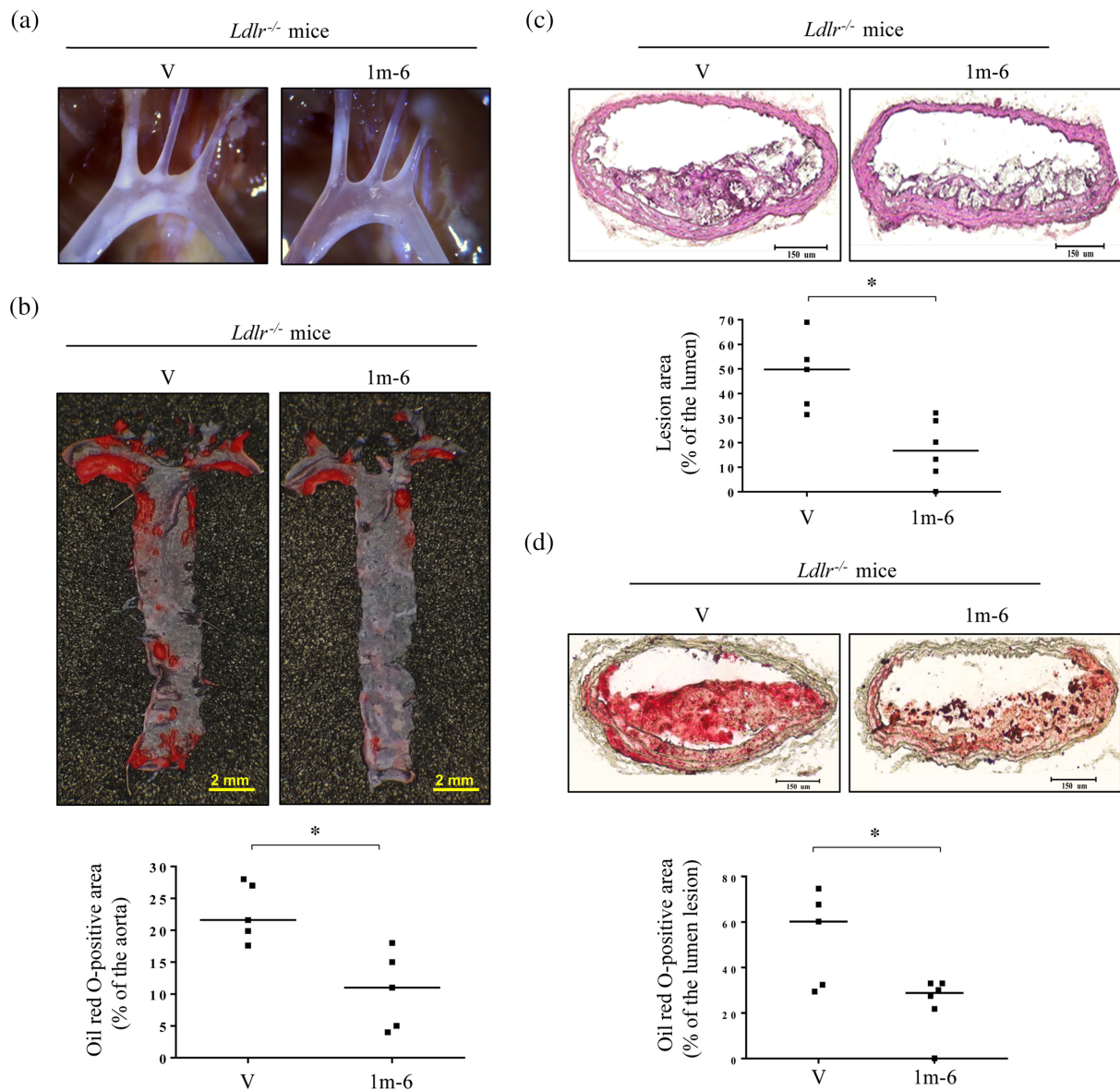


FIGURE 7 Treatment with 1m-6 attenuates lipid accumulation and plaque formation in atherosclerosis-prone mice. (a) Representative light microscopy pictures of the 1m-6-treated ($n = 6$) or DMSO-treated ($n = 5$) aortic arches in LDL receptor knockout ($Ldlr^{-/-}$) mice fed a high-fat diet (HFD). (b) Representative en face ORO staining and quantitative results of the 1m-6-treated ($n = 6$) or DMSO-treated ($n = 5$) whole aortas from $Ldlr^{-/-}$ mice fed an HFD. (c and d) Representative histological analysis and quantitative results of sliced arteries from 1m-6-treated ($n = 6$) or DMSO-treated ($n = 5$) $Ldlr^{-/-}$ mice fed an HFD with haematoxylin and eosin (H&E) staining (c) and ORO staining (d). The results are expressed as the median with individual data. Significance is presented as $^*P < 0.05$ versus the indicated group

extensively reduces the expression of miRNAs-regulating ABCA1 expression, which further protects ABCA1 mRNA from degradation. This evidence highlights the potent effects of 1m-6 on the post-translational regulation of ABCA1 expression.

The atheroprotective effects of HO-1 have been proposed to be related to its anti-inflammatory and antioxidant properties (Abraham, Junge, & Drummond, 2016). Depletion of HO-1 has been shown to abrogate up-regulation of ABCA1 expression in *Ginkgo biloba* extract 761- or tanshinone IIA-treated macrophages (Liu et al., 2014; Tsai et al., 2010), which indicates that HO-1 plays a role in the protection of ABCA1 protein from degradation. Interestingly, we found that

under 1m-6 treatment, HO-1 signalling suppresses the expression ABCA1-regulating miRNAs, which possibly further enhances ABCA1 mRNA stability. In contrast to the studies with *G. biloba* extract 761- or tanshinone IIA-treated macrophages, we propose that HO-1 might participate in the biosynthesis of these ABCA1-regulating miRNAs in 1m-6-treated THP-1 macrophages. HO-1 is an antioxidative and cytoprotective enzyme, which degrades haem to biliverdin, iron ions and carbon monoxide (Maines, 1997). Previous studies indicated that overexpression of HO-1 reduced DGCR8 dimer formation and expression of DGCR8, which is a protein involved in miRNA processing and requires

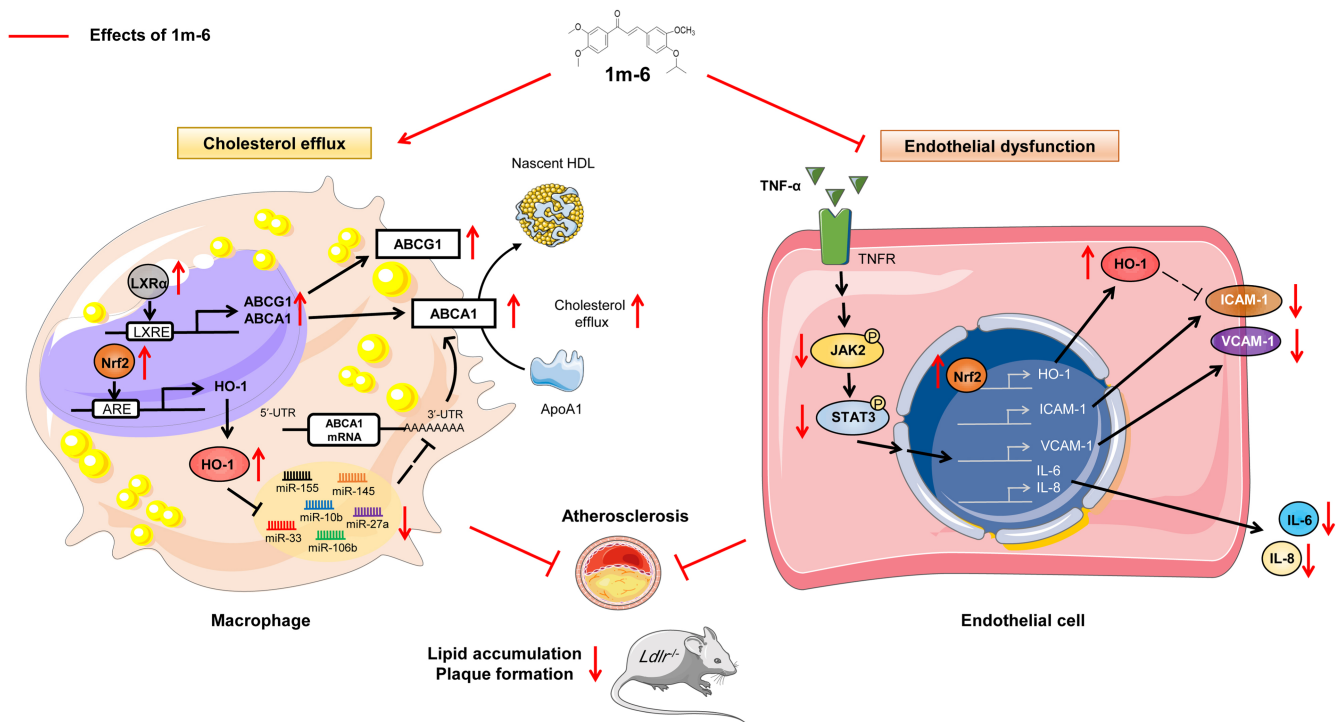


FIGURE 8 Schematic diagram of the antiatherogenic effects of 1m-6 in THP-1 macrophages, TNF- α -activated human umbilical vein endothelial cells (HUVECs) and atherosclerosis-prone mice. Treatment with 1m-6 increases ABCA1 expression and promotes cholesterol efflux in human THP-1 macrophages and inhibits TNF- α -induced adhesion molecule and inflammatory mediator expression in HUVECs, thereby contributing to the atheroprotective effects in atherosclerosis-prone mice. In human THP-1 macrophages, 1m-6 enhances ABCA1 expression by activating LXR α and Nrf2/HO-1 signalling. Treatment with 1m-6 down-regulates the expression of ABCA1-regulating miRNAs through the modulation of HO-1 expression. In HUVECs, 1m-6 suppresses TNF- α -induced VCAM-1 and ICAM-1 expression through the inhibition of JAK/STAT3 activation and the up-regulation of Nrf2/HO-1 expression, respectively

haem, leading to disturbed miRNA production (Ameres & Zamore, 2013; Kozakowska et al., 2012). Such evidence partly explained the effects of 1m-6 on the up-regulation of HO-1 and down-regulation of ABCA1-regulating miRNAs. Further studies are needed to clarify the role of 1m-6 on HO-1 up-regulation and miRNA expression.

Our study demonstrates that 1m-6 treatment suppresses TNF- α -induced VCAM-1 and ICAM-1 expression in HUVECs. Previous studies suggested that viscolin, a chalcone isolated from *Viscum coloratum*, inhibits TNF- α -induced VCAM-1 expression by suppressing JNK-NF- κ B signalling (Liang et al., 2011). Interestingly, 1m-6 inhibits the TNF- α -induced expression of VCAM-1 and ICAM-1 via down-regulation of STAT3 activation and up-regulation of HO-1 expression in endothelial cells, respectively, but does not affect NF- κ B signalling. Although viscolin and 1m-6 are chalcone derivatives, they have distinct separate mechanisms on the regulation of TNF- α -induced adhesion molecules. Consistent with our results, **cinnamaldehyde** has been shown to exert inhibitory effects on TNF- α -induced ICAM-1 expression through HO-1 signalling in endothelial cells (Liao et al., 2008). Additionally, 1m-6 suppressed the production of proinflammatory cytokines, such as IL-6 and IL-8, in TNF- α -activated HUVECs, which further emphasizes the anti-inflammatory and atheroprotective nature of 1m-6 (Bhaskar et al., 2011).

Treatment with 1m-6 suppresses VCAM-1 expression by interfering with JAK/STAT3 signalling in TNF- α -stimulated endothelial cells. STAT3 plays crucial roles in the development of atherosclerosis through the regulation of vascular cells, including endothelial cells, vascular smooth muscle cells and immune cells (Chen et al., 2019). Importantly, mice with endothelial-specific STAT3 ablation exhibit reduced atherosclerotic lesions (Gharavi et al., 2007). Previous studies have shown that STAT3 plays a role in the development of endothelial dysfunction via the rearrangement of microfilaments and microtubules and regulation of adhesion molecule expression (Chen et al., 2019). Sustained STAT3 activation contributes to the unregulated expression of adhesion molecules in endothelial cells. Consistent with our results, previous studies suggested that pharmacological or genetic inhibition of STAT3 activation suppresses TNF- α -induced VCAM-1 expression (Lee et al., 2012; Liu et al., 2017). Although it has been proposed that chalcone derivatives inhibit STAT3 signalling in haematopoietic and pancreatic cells (Funakoshi-Tago et al., 2008; Jiang et al., 2015), we provide the first evidence that 1m-6 attenuates TNF- α -induced VCAM-1 expression through STAT3 signalling in endothelial cells. Intriguingly, our results suggest that the genetic inhibition of STAT3 represses the expression of VCAM-1 in TNF- α -stimulated endothelial cells to a lesser extent than 1m-6 treatment. The incomplete depletion of STAT3 in this study and the other

possible regulatory mechanisms involved in the 1m-6-mediated modulation of VCAM-1 expression partly explain the above-mentioned effects of STAT3 and 1m-6 on VCAM-1 expression.

We first identified a chalcone derivative, 1m-6, that significantly ameliorates atherosclerotic plaque and lipid accumulation in the aortas of *Ldlr*^{-/-} mice fed a high-fat diet. Several *in vivo* immunomodulatory effects of chalcone derivatives have been studied. The novel chalcone derivative, L2H17, protects mice fed an high-fat diet against obesity-induced renal injury (Fang, Deng, et al., 2015) and reduces the inflammatory response in the heart and kidney of streptozotocin-induced diabetic mice (Fang, Wang, et al., 2015). Treatment with hesperidin methyl chalcone, a chalcone derivative, inhibits hyperalgesia and the inflammatory response induced by carrageenan and complete Freund's adjuvant in Swiss mice (Pinho-Ribeiro et al., 2015). Regarding the cardioprotective effects of chalcone derivatives, it has been suggested that the administration of trans-chalcone improves atherogenesis, liver fibrosis and lipid profiles in NMRI mice fed an high-fat diet (Karkhaneh, Yaghmaei, Parivar, Sadeghizadeh, & Ebrahim-Habibi, 2016) via unclear mechanisms. Using immunohistochemistry staining, we found that treatment with 1m-6 reduced the expression of CD68 in the atherosclerotic plaques of *Ldlr*^{-/-} mice (data not shown). These results indicate the anti-inflammatory nature of 1m-6 with the inhibition of macrophages infiltration during 1m-6 treatment, which is another important underlying mechanism of antiatherosclerotic effects of 1m-6. Interestingly, 1m-6 did not affect ABCA1 expression in the atherosclerotic plaques. Discrepancies between the *in vitro* and *in vivo* effects of 1m-6 on ABCA1 expression may be due to the decreased number of macrophages in atherosclerotic plaques. Using biologically functional approaches and the genetic inhibition of HO-1 and STAT3, we demonstrate the remarkable therapeutic effects of 1m-6 in atherosclerosis-prone *Ldlr*^{-/-} mice and provide mechanistic insights into its atheroprotective effects.

Several limitations should be mentioned. First, the *in vivo* cholesterol efflux effect of 1m-6 was not assessed in the current study. Second, genetic manipulations of ABCA1, HO-1 and STAT3 in mice treated with 1m-6, which would powerfully elucidate the mechanisms regarding 1m-6 effects on atherosclerosis, were not conducted. Third, the effects of STAT3 inhibitors on vascular cell function and atherosclerosis were not evaluated. Finally, the underlying regulatory mechanisms regarding 1m-6 on Nrf2/HO-1 signalling require further evaluation. **Kelch-like ECH-associated protein 1** is a repressor protein that binds to Nrf2 and promotes its degradation. The conformation change of kelch-like ECH-associated protein 1 results in nuclear translocation of Nrf2 and subsequent target gene expression (Kansanen, Kuosmanen, Leinonen, & Levonen, 2013; Taguchi, Motohashi, & Yamamoto, 2011). Accordingly, the effects of 1m-6 on kelch-like ECH-associated protein 1 inhibition require further investigation in future studies. Despite these limitations, our study clearly shows the promising atheroprotective effects of 1m-6.

In conclusion, we developed a novel and potent chalcone derivative, 1m-6, with the dual-atheroprotective effects of enhancing cholesterol efflux and reducing inflammation-induced endothelial dysfunction. The enhancement of cholesterol efflux and ABCA1

expression by 1m-6 in macrophages occurs through Nrf2/HO-1-miRNA signalling. Additionally, 1m-6 attenuates TNF- α -induced VCAM-1 and ICAM-1 expression in HUVECs by suppressing JAK/STAT3 and promoting Nrf2/HO-1 signalling, respectively. In addition to exhibiting promising atheroprotective effects in *Ldlr*^{-/-} mice, 1m-6 exhibits therapeutic potential for atherosclerotic cardiovascular disease. Further *in vivo* and human studies are needed to confirm the atheroprotective effects of 1m-6.

ACKNOWLEDGEMENTS

We thank Professor Carlos Fernandez-Hernando and Professor Shih-Ming Huang for their invaluable comments. We also thank I-Jou Teng, Yi-Jhen Huang, Shao-Fu Shih and Pei-Wen Liu for their skilful technical assistance. This work is supported by grants from Tri-Service General Hospital (TSGH-C107-007-007-S02, TSGH-C108-006-007-007-S02 and TSGH-E-109206 to C.-S.L. and TSGH-E-109218 and TSGH C108-069 to S.-J.C.), Ministry of National Defense-Medical Affairs Bureau (MAB-106-082 to C.-S.L. and MAB-106-102 and MAB-109-069 to M.-C.T.) and Taiwan Ministry of Science and Technology (MOST 105-2325-B016-001 and MOST 106-2320-B-016-010 to M.-C.T. and MOST 106-2314-B-016-038-MY3 and MOST 108-3111-Y-016-015 to C.-S.L.).

AUTHOR CONTRIBUTIONS

L.W.C., M.-C.T. and C.-S.L. participated in the research design. C.-Y.C. and H.-J.L. synthesized chalcone derivatives. L.W.C., B.-F.T., Y.-W.L., M.-C.T., S.-J.C., F.-Y.L. and C.-S.L. performed the experiments. L.W.C., Y.-W.L., C.-S.L. and M.-C.T. performed data analysis. L.W.C., M.-C.T., C.-Y.C. and C.-S.L. wrote the manuscript. L.W.C., C.-Y.C., M.-C.T., T.-P. T., C.-S.T., S.-J.C., W.-L.W., W.-S.L. and C.-S.L. contributed to the editing of the manuscript and the funding for purchasing of materials and reagents. C.-S.L. is the principal investigator of this project.

CONFLICT OF INTEREST

The authors declare no conflict of interest.

DECLARATION OF TRANSPARENCY AND SCIENTIFIC RIGOUR

This Declaration acknowledges that this paper adheres to the principles for transparent reporting and scientific rigour of preclinical research as stated in the *BJP* guidelines for [Design & Analysis](#), [Immunoblotting and Immunochemistry](#) and [Animal Experimentation](#), and as recommended by funding agencies, publishers and other organizations engaged with supporting research.

DATA AVAILABILITY STATEMENT

The data that support the findings of this study are available from the corresponding author upon reasonable request. Some data may not be made available because of privacy or ethical restrictions.

ORCID

Liv Weichien Chen  <https://orcid.org/0000-0001-6759-0023>

Chin-Sheng Lin  <https://orcid.org/0000-0002-5167-8327>

REFERENCES

- Abraham, N. G., Junge, J. M., & Drummond, G. S. (2016). Translational significance of heme oxygenase in obesity and metabolic syndrome. *Trends in Pharmacological Sciences*, *37*, 17–36. <https://doi.org/10.1016/j.tips.2015.09.003>
- Alexander, S. P. H., Roberts, R. E., Broughton, B. R. S., Sobey, C. G., George, C. H., Stanford, S. C., ... Ahluwalia, A. (2018). Goals and practicalities of immunoblotting and immunohistochemistry: A guide for submission to the *British Journal of Pharmacology*. *British Journal of Pharmacology*, *175*, 407–411. <https://doi.org/10.1111/bph.14112>
- Alexander, S. P. H., Kelly, E., Mathie, A., Peters, J. A., Veale, E. L., Armstrong, J. F., ... Southan, C. (2019). The Concise Guide to PHARMACOLOGY 2019/20: Introduction and Other Protein Targets. *British Journal of Pharmacology*, *176*(Suppl 1), S1–S20. <https://doi.org/10.1111/bph.14747>
- Ameres, S. L., & Zamore, P. D. (2013). Diversifying microRNA sequence and function. *Nature Reviews. Molecular Cell Biology*, *14*, 475–488. <https://doi.org/10.1038/nrm3611>
- Annapurna, A., Mudagal, M. P., Ansari, A., & Rao, A. S. (2012). Cardioprotective activity of chalcones in ischemia/reperfusion-induced myocardial infarction in albino rats. *Experimental and Clinical Cardiology*, *17*, 110–114.
- Baselga-Escudero, L., Blade, C., Ribas-Latre, A., Casanova, E., Suarez, M., Torres, J. L., ... Arola-Arnal, A. (2014). Resveratrol and EGCG bind directly and distinctively to miR-33a and miR-122 and modulate divergently their levels in hepatic cells. *Nucleic Acids Research*, *42*, 882–892. <https://doi.org/10.1093/nar/gkt1011>
- Bensinger, S. J., & Tontonoz, P. (2008). Integration of metabolism and inflammation by lipid-activated nuclear receptors. *Nature*, *454*, 470–477. <https://doi.org/10.1038/nature07202>
- Bhaskar, V., Yin, J., Mirza, A. M., Phan, D., Vanegas, S., Issafiras, H., ... Kantak, S. S. (2011). Monoclonal antibodies targeting IL-1 beta reduce biomarkers of atherosclerosis *in vitro* and inhibit atherosclerotic plaque formation in Apolipoprotein E-deficient mice. *Atherosclerosis*, *216*, 313–320. <https://doi.org/10.1016/j.atherosclerosis.2011.02.026>
- Canfran-Duque, A., Lin, C. S., Goedeke, L., Suarez, Y., & Fernandez-Hernando, C. (2016). Micro-RNAs and high-density lipoprotein metabolism. *Arteriosclerosis, Thrombosis, and Vascular Biology*, *36*, 1076–1084. <https://doi.org/10.1161/ATVBAHA.116.307028>
- Canfran-Duque, A., Ramirez, C. M., Goedeke, L., Lin, C. S., & Fernandez-Hernando, C. (2014). microRNAs and HDL life cycle. *Cardiovascular Research*, *103*, 414–422. <https://doi.org/10.1093/cvr/cvu140>
- Chen, C. W., Wang, L. L., Zaman, S., Gordon, J., Arisi, M. F., Venkataraman, C. M., ... Atluri, P. (2018). Sustained release of endothelial progenitor cell-derived extracellular vesicles from shear-thinning hydrogels improves angiogenesis and promotes function after myocardial infarction. *Cardiovascular Research*, *114*, 1029–1040. <https://doi.org/10.1093/cvr/cvy067>
- Chen, Q., Lv, J., Yang, W., Xu, B., Wang, Z., Yu, Z., ... Han, Y. (2019). Targeted inhibition of STAT3 as a potential treatment strategy for atherosclerosis. *Theranostics*, *9*, 6424–6442. <https://doi.org/10.7150/thno.35528>
- Chen, S. J., Kao, Y. H., Jing, L., Chuang, Y. P., Wu, W. L., Liu, S. T., ... Lin, C. S. (2017). Epigallocatechin-3-gallate reduces scavenger receptor A expression and foam cell formation in human macrophages. *Journal of Agricultural and Food Chemistry*, *65*, 3141–3150. <https://doi.org/10.1021/acs.jafc.6b05832>
- Chen, Y. H., Wang, W. H., Wang, Y. H., Lin, Z. Y., Wen, C. C., & Chern, C. Y. (2013). Evaluation of the anti-inflammatory effect of chalcone and chalcone analogues in a zebrafish model. *Molecules*, *18*, 2052–2060. <https://doi.org/10.3390/molecules18022052>
- Curtis, M. J., Alexander, S., Cirino, G., Docherty, J. R., George, C. H., Giembycz, M. A., ... Ahluwalia, A. (2018). Experimental design and analysis and their reporting II: Updated and simplified guidance for authors and peer reviewers. *British Journal of Pharmacology*, *175*, 987–993. <https://doi.org/10.1111/bph.14153>
- Cybulsky, M. I., Iiyama, K., Li, H., Zhu, S., Chen, M., Iiyama, M., ... Milstone, D. S. (2001). A major role for VCAM-1, but not ICAM-1, in early atherosclerosis. *The Journal of Clinical Investigation*, *107*, 1255–1262. <https://doi.org/10.1172/JCI11871>
- Daiber, A., Steven, S., Weber, A., Shuvaev, V. V., Muzykantov, V. R., Laher, I., ... Münzel, T. (2017). Targeting vascular (endothelial) dysfunction. *British Journal of Pharmacology*, *174*, 1591–1619. <https://doi.org/10.1111/bph.13517>
- Fang, Q., Deng, L., Wang, L., Zhang, Y., Weng, Q., Yin, H., ... Liang, G. (2015). Inhibition of mitogen-activated protein kinases/nuclear factor κ B-dependent inflammation by a novel chalcone protects the kidney from high fat diet-induced injuries in mice. *The Journal of Pharmacology and Experimental Therapeutics*, *355*, 235–246. <https://doi.org/10.1124/jpet.115.226860>
- Fang, Q., Wang, J., Wang, L., Zhang, Y., Yin, H., Li, Y., ... Zheng, C. (2015). Attenuation of inflammatory response by a novel chalcone protects kidney and heart from hyperglycemia-induced injuries in type 1 diabetic mice. *Toxicology and Applied Pharmacology*, *288*, 179–191. <https://doi.org/10.1016/j.taap.2015.07.009>
- Fiedler, U., Reiss, Y., Scharpfenecker, M., Grunow, V., Koidl, S., Thurston, G., ... Augustin, H. G. (2006). Angiotensin-2 sensitizes endothelial cells to TNF- α and has a crucial role in the induction of inflammation. *Nature Medicine*, *12*, 235–239. <https://doi.org/10.1038/nm1351>
- Funakoshi-Tago, M., Tago, K., Nishizawa, C., Takahashi, K., Mashino, T., Iwata, S., ... Kasahara, T. (2008). Licochalcone A is a potent inhibitor of TEL-Jak2-mediated transformation through the specific inhibition of Stat3 activation. *Biochemical Pharmacology*, *76*, 1681–1693. <https://doi.org/10.1016/j.bcp.2008.09.012>
- Gharavi, N. M., Alva, J. A., Mouillesseaux, K. P., Lai, C., Yeh, M., Yeung, W., ... Berliner, J. A. (2007). Role of the Jak/STAT pathway in the regulation of interleukin-8 transcription by oxidized phospholipids *in vitro* and in atherosclerosis *in vivo*. *The Journal of Biological Chemistry*, *282*, 31460–31468. <https://doi.org/10.1074/jbc.M704267200>
- Gistera, A., & Hansson, G. K. (2017). The immunology of atherosclerosis. *Nature Reviews. Nephrology*, *13*, 368–380. <https://doi.org/10.1038/nrneph.2017.51>
- Harding, S. D., Sharman, J. L., Faccenda, E., Southan, C., Pawson, A. J., Ireland, S., ... NC-IUPHAR. (2018). The IUPHAR/BPS Guide to PHARMACOLOGY in 2018: Updates and expansion to encompass the new guide to IMMUNOPHARMACOLOGY. *Nucleic Acids Research*, *46*, D1091–D1106. <https://doi.org/10.1093/nar/gkx1121>
- Ishibashi, S., Brown, M. S., Goldstein, J. L., Gerard, R. D., Hammer, R. E., & Herz, J. (1993). Hypercholesterolemia in low density lipoprotein receptor knockout mice and its reversal by adenovirus-mediated gene delivery. *The Journal of Clinical Investigation*, *92*, 883–893. <https://doi.org/10.1172/JCI116663>
- Itoh, K., Chiba, T., Takahashi, S., Ishii, T., Igarashi, K., Katoh, Y., ... Nabeshima, Y. I. (1997). An Nrf2/small Maf heterodimer mediates the induction of phase II detoxifying enzyme genes through antioxidant response elements. *Biochemical and Biophysical Research Communications*, *236*, 313–322. <https://doi.org/10.1006/bbrc.1997.6943>
- Jiang, W., Zhao, S., Xu, L., Lu, Y., Lu, Z., Chen, C., ... Yang, L. (2015). The inhibitory effects of xanthohumol, a prenylated chalcone derived from hops, on cell growth and tumorigenesis in human pancreatic cancer. *Biomedicine & Pharmacotherapy*, *73*, 40–47. <https://doi.org/10.1016/j.biopha.2015.05.020>
- Kandhaya-Pillai, R., Miro-Mur, F., Alijotas-Reig, J., Tchkonja, T., Kirkland, J. L., & Schwartz, S. (2017). TNF α -senescence initiates a STAT-dependent positive feedback loop, leading to a sustained interferon signature, DNA damage, and cytokine secretion. *Aging (Albany NY)*, *9*, 2411–2435. <https://doi.org/10.18632/aging.101328>
- Kang, M. H., Zhang, L. H., Wijesekara, N., de Haan, W., Butland, S., Bhattacharjee, A., & Hayden, M. R. (2013). Regulation of ABCA1 protein expression and function in hepatic and pancreatic islet cells by

- miR-145. *Arteriosclerosis, Thrombosis, and Vascular Biology*, 33, 2724–2732. <https://doi.org/10.1161/ATVBAHA.113.302004>
- Kansanen, E., Kuosmanen, S. M., Leinonen, H., & Levonen, A. L. (2013). The Keap1-Nrf2 pathway: Mechanisms of activation and dysregulation in cancer. *Redox Biology*, 1, 45–49. <https://doi.org/10.1016/j.redox.2012.10.001>
- Karkhaneh, L., Yaghmaei, P., Parivar, K., Sadeghizadeh, M., & Ebrahim-Habibi, A. (2016). Effect of trans-chalcone on atheroma plaque formation, liver fibrosis and adiponectin gene expression in cholesterol-fed NMRI mice. *Pharmacological Reports*, 68, 720–727. <https://doi.org/10.1016/j.pharep.2016.03.004>
- Khera, A. V., Cuchel, M., de la Llera-Moya, M., Rodrigues, A., Burke, M. F., Jafri, K., ... Rader, D. J. (2011). Cholesterol efflux capacity, high-density lipoprotein function, and atherosclerosis. *The New England Journal of Medicine*, 364, 127–135. <https://doi.org/10.1056/NEJMoa1001689>
- Kilkenny, C., Browne, W. J., Cuthill, I. C., Emerson, M., & Altman, D. G. (2010). Improving bioscience research reporting: The ARRIVE guidelines for reporting animal research. *PLoS Biology*, 8, e1000412. <https://doi.org/10.1371/journal.pbio.1000412>
- Kozakowska, M., Ciesla, M., Stefanska, A., Skrzypek, K., Was, H., Jazwa, A., ... Jozkowicz, A. (2012). Heme oxygenase-1 inhibits myoblast differentiation by targeting myomirs. *Antioxidants & Redox Signaling*, 16, 113–127. <https://doi.org/10.1089/ars.2011.3964>
- Lee, J. E., Lee, A. S., Kim, D. H., Jung, Y. J., Lee, S., Park, B. H., ... Kang, K. P. (2012). Janex-1, a JAK3 inhibitor, ameliorates tumor necrosis factor- α -induced expression of cell adhesion molecules and improves myocardial vascular permeability in endotoxemic mice. *International Journal of Molecular Medicine*, 29, 864–870. <https://doi.org/10.3892/ijmm.2012.920>
- Liang, C. J., Wang, S. H., Chen, Y. H., Chang, S. S., Hwang, T. L., Leu, Y. L., ... Chen, Y. L. (2011). Viscolin reduces VCAM-1 expression in TNF- α -treated endothelial cells via the JNK/NF- κ B and ROS pathway. *Free Radical Biology & Medicine*, 51, 1337–1346. <https://doi.org/10.1016/j.freeradbiomed.2011.06.023>
- Liao, B. C., Hsieh, C. W., Liu, Y. C., Tzeng, T. T., Sun, Y. W., & Wung, B. S. (2008). Cinnamaldehyde inhibits the tumor necrosis factor- α -induced expression of cell adhesion molecules in endothelial cells by suppressing NF- κ B activation: Effects upon I κ B and Nrf2. *Toxicology and Applied Pharmacology*, 229, 161–171. <https://doi.org/10.1016/j.taap.2008.01.021>
- Liu, Y. S., Lin, H. Y., Lai, S. W., Huang, C. Y., Huang, B. R., Chen, P. Y., ... Lu, D. Y. (2017). MiR-181b modulates EGFR-dependent VCAM-1 expression and monocyte adhesion in glioblastoma. *Oncogene*, 36, 5006–5022. <https://doi.org/10.1038/ncr.2017.129>
- Liu, Z., Wang, J., Huang, E., Gao, S., Li, H., Lu, J., ... Liu, P. (2014). Tanshinone IIA suppresses cholesterol accumulation in human macrophages: Role of heme oxygenase-1. *Journal of Lipid Research*, 55, 201–213. <https://doi.org/10.1194/jlr.M040394>
- Lv, Y. C., Yang, J., Yao, F., Xie, W., Tang, Y. Y., Ouyang, X. P., ... Tang, C. K. (2015). Diosgenin inhibits atherosclerosis via suppressing the MiR-19b-induced downregulation of ATP-binding cassette transporter A1. *Atherosclerosis*, 240, 80–89. <https://doi.org/10.1016/j.atherosclerosis.2015.02.044>
- Ma, Y., Xu, L., Rodriguez-Agudo, D., Li, X., Heuman, D. M., Hylemon, P. B., ... Ren, S. (2008). 25-Hydroxycholesterol-3-sulfate regulates macrophage lipid metabolism via the LXR/SREBP-1 signaling pathway. *American Journal of Physiology. Endocrinology and Metabolism*, 295, E1369–E1379. <https://doi.org/10.1152/ajpendo.90555.2008>
- Macias, C., Villaescusa, R., del Valle, L., Boffil, V., Cordero, G., Hernandez, A., & Ballester, J. M. (2003). Endothelial adhesion molecules ICAM-1, VCAM-1 and E-selectin in patients with acute coronary syndrome. *Revista Española de Cardiología*, 56, 137–144. [https://doi.org/10.1016/S0300-8932\(03\)76837-7](https://doi.org/10.1016/S0300-8932(03)76837-7)
- Maines, M. D. (1997). The heme oxygenase system: A regulator of second messenger gases. *Annual Review of Pharmacology and Toxicology*, 37, 517–554. <https://doi.org/10.1146/annurev.pharmtox.37.1.517>
- McGrath, J. C., Pawson, A. J., Sharman, J. L., & Alexander, S. P. (2015). BJP is linking its articles to the IUPHAR/BPS Guide to PHARMACOLOGY. *British Journal of Pharmacology*, 172, 2929–2932. <https://doi.org/10.1111/bph.13112>
- Padhye, S., Ahmad, A., Oswal, N., & Sarkar, F. H. (2009). Emerging role of Garcinol, the antioxidant chalcone from *Garcinia indica* Choisy and its synthetic analogs. *Journal of Hematology & Oncology*, 2, 38. <https://doi.org/10.1186/1756-8722-2-38>
- Patten, R. D. (2007). Models of gender differences in cardiovascular disease. *Drug Discov Today Dis Models*, 4, 227–232. <https://doi.org/10.1016/j.ddmod.2007.11.002>
- Phillips, M. C. (2014). Molecular mechanisms of cellular cholesterol efflux. *The Journal of Biological Chemistry*, 289, 24020–24029. <https://doi.org/10.1074/jbc.R114.583658>
- Pinho-Ribeiro, F. A., Hohmann, M. S., Borghi, S. M., Zarpelon, A. C., Guazelli, C. F., Manchope, M. F., ... Verri, W. A. Jr. (2015). Protective effects of the flavonoid hesperidin methyl chalcone in inflammation and pain in mice: Role of TRPV1, oxidative stress, cytokines and NF- κ B. *Chemico-Biological Interactions*, 228, 88–99. <https://doi.org/10.1016/j.cbi.2015.01.011>
- Price, N. L., Rotllan, N., Zhang, X., Canfran-Duque, A., Nottoli, T., Suarez, Y., & Fernández-Hernando, C. (2019). Specific disruption of Abca1 targeting largely mimics the effects of miR-33 knockout on macrophage cholesterol efflux and atherosclerotic plaque development. *Circulation Research*, 124, 874–880. <https://doi.org/10.1161/CIRCRESAHA.118.314415>
- Ramirez, C. M., Davalos, A., Goedeke, L., Salerno, A. G., Warriar, N., Cirera-Salinas, D., ... Fernández-Hernando, C. (2011). MicroRNA-758 regulates cholesterol efflux through posttranscriptional repression of ATP-binding cassette transporter A1. *Arteriosclerosis, Thrombosis, and Vascular Biology*, 31, 2707–2714. <https://doi.org/10.1161/ATVBAHA.111.232066>
- Rohatgi, A., Khera, A., Berry, J. D., Givens, E. G., Ayers, C. R., Wedin, K. E., ... Shaul, P. W. (2014). HDL cholesterol efflux capacity and incident cardiovascular events. *The New England Journal of Medicine*, 371, 2383–2393. <https://doi.org/10.1056/NEJMoa1409065>
- Romaine, S. P., Tomaszewski, M., Condorelli, G., & Samani, N. J. (2015). MicroRNAs in cardiovascular disease: An introduction for clinicians. *Heart*, 101, 921–928. <https://doi.org/10.1136/heartjnl-2013-305402>
- Satoh, T., Okamoto, S. I., Cui, J., Watanabe, Y., Furuta, K., Suzuki, M., ... Lipton, S. A. (2006). Activation of the Keap1/Nrf2 pathway for neuroprotection by electrophilic [correction of electrophilic] phase II inducers. *Proceedings of the National Academy of Sciences of the United States of America*, 103, 768–773. <https://doi.org/10.1073/pnas.0505723102>
- Soares, M. P., Seldon, M. P., Gregoire, I. P., Vassilevskaia, T., Berberat, P. O., Yu, J., ... Bach, F. H. (2004). Heme oxygenase-1 modulates the expression of adhesion molecules associated with endothelial cell activation. *Journal of Immunology*, 172, 3553–3563. <https://doi.org/10.4049/jimmunol.172.6.3553>
- Taguchi, K., Motohashi, H., & Yamamoto, M. (2011). Molecular mechanisms of the Keap1-Nrf2 pathway in stress response and cancer evolution. *Genes to Cells*, 16, 123–140. <https://doi.org/10.1111/j.1365-2443.2010.01473.x>
- Teng, I. J., Tsai, M. C., Shih, S. F., Tsuei, B. F., Chang, H., Chuang, Y. P., ... Chen, S. J. (2018). Chalcone derivatives enhance ATP-binding cassette transporters A1 in human THP-1 macrophages. *Molecules*, 23, 1620. <https://doi.org/10.3390/molecules23071620>
- Tsai, J. Y., Su, K. H., Shyue, S. K., Kou, Y. R., Yu, Y. B., Hsiao, S. H., ... Lee, T. S. (2010). EGb761 ameliorates the formation of foam cells by

- regulating the expression of SR-A and ABCA1: Role of haem oxygenase-1. *Cardiovascular Research*, 88, 415–423. <https://doi.org/10.1093/cvr/cvq226>
- Yang, D., Wang, P., Liu, J., Xing, H., Liu, Y., Xie, W., & Zhao, G. (2014). Design, synthesis and evaluation of novel indole derivatives as AKT inhibitors. *Bioorganic & Medicinal Chemistry*, 22, 366–373. <https://doi.org/10.1016/j.bmc.2013.11.022>
- Zelcer, N., & Tontonoz, P. (2006). Liver X receptors as integrators of metabolic and inflammatory signaling. *The Journal of Clinical Investigation*, 116, 607–614. <https://doi.org/10.1172/JCI27883>
- Zhao, X., Dong, W., Gao, Y., Shin, D. S., Ye, Q., Su, L., ... Miao, J. Y. (2017). Novel indolyl-chalcone derivatives inhibit A549 lung cancer cell growth through activating Nrf-2/HO-1 and inducing apoptosis in vitro and in vivo. *Scientific Reports*, 7, 3919. <https://doi.org/10.1038/s41598-017-04411-3>
- Zhuang, C., Zhang, W., Sheng, C., Zhang, W., Xing, C., & Miao, Z. (2017). Chalcone: A privileged structure in medicinal chemistry. *Chemical*

Reviews, 117, 7762–7810. <https://doi.org/10.1021/acs.chemrev.7b00020>

SUPPORTING INFORMATION

Additional supporting information may be found online in the Supporting Information section at the end of this article.

How to cite this article: Chen LW, Tsai M-C, Chen C-Y, et al. A chalcone derivative, 1m-6, exhibits atheroprotective effects by increasing cholesterol efflux and reducing inflammation-induced endothelial dysfunction. *Br J Pharmacol*. 2020;177:5375–5392. <https://doi.org/10.1111/bph.15175>